the TiO_2 NPs as a sonocatalyst [28,29]. However, these reports did not examine the detailed kinetics of TiO_2 NPs uptake by the cancer cells and the prolonged effect of SDT using the TiO_2 NPs on the cell viability *in vitro*.

Therefore, in the present study, the efficacy of the SDT using protein-immobilized TiO_2 NPs (called TiO_2/US treatment) was examined *in vitro* and *in vivo*. This study specifically examines the uptake behavior of TiO_2 NPs modified with pre-S1/S2 (part of the L protein from the hepatitis B virus with high affinity to hepatocyte [30]) by HepG2 cells. Moreover, this study examines the effect of the TiO_2/US treatment on apoptosis induction in the early stage and the subsequent growth behavior of cancer cells. Lastly, the TiO_2/US treatment was tested *in vivo* using a mouse xenograft model.

2. Materials and methods

2.1. Pre-S1/S2-immobilized TiO_2 NPs

Suspension of TiO_2 NPs (MPT-422, Ishihara Sangyo Kaisha, Ltd., Osaka, Japan) was used as starting materials for preparing Pre-S1/S2-immobilized TiO_2 NPs. The recombinant fusion proteins GST-GFP and GST-GFP-pre-S1/S2 were prepared using *Escherichia coli* BL21(DE3) harboring plasmid pGEX-GFP or pGEX-GFP-pre-S1/S2 [31] as per the procedure described previously [27]. The chemicals used in this study were of guaranteed reagent grade without further purification.

Surface of the TiO_2 NPs was modified by polyacrylic acids (PAA) as described previously to avoid aggregation of TiO_2 NPs under physiologic conditions [32]. The GST-GFP or GST-GFP-pre-S1/S2 protein was immobilized on the surface of the PAA-modified TiO_2 NPs by chemical coupling at the carboxyl residue, using 1-ethyl-3-(3-dimethylaminopropyl) carbodiimide hydrochloride and *N*-hydroxysuccinimide (Wako Pure Chemical Industries, Osaka, Japan) [27,32]. The resultant NPs (120 nm in average size [27]) were designated as GFP-TiO_2 NPs and pre-S1/S2-GFP-TiO_2 NPs, respectively, in the present study.

2.2. Cell culture and animals

Human hepatoma HepG2 cells were used as model cancer cells throughout the study. When necessary, human colon carcinoma cells WiDr were also used. The HepG2 cells were cultured in Dulbecco's modified Eagle medium (DMEM, Nakarai Tesqu, Kyoto, Japan) supplemented with 10% (v/v) fetal bovine serum (FBS; Invitrogen GIBCO, Carlsbad, CA, USA), 60 μg/ml penicillin (Nakarai Tesqu, Kyoto, Japan), and 100 μg/ml streptomycin (Nakarai Tesqu, Kyoto, Japan). The cells were maintained at 37 °C and under a 5% CO_2 atmosphere.

BALB/c nude mice were used to prepare the xenograft model. The mice were housed in a controlled environment at 22 °C on 12 h light/dark cycles. The mice were 5 weeks old at the beginning of the experiments, weighing 22–25 g. The experimental animals were treated according to the standards supported by the animal protection committee of Kanazawa University.

2.3. TiO_2/US treatment in vitro

For the *in vitro* experiments, 4×10^5 HepG2 cells suspended in 2 ml DMEM were seeded in 35-mm culture dishes and incubated for 24 h. The pre-S1/S2-GFP-TiO_2 NPs suspension was added to the culture medium at a final concentration of 0.01% (w/v) and incubated for an additional 0–24 h. Pre-S1/S2 mediated uptake of the TiO_2 NPs by HepG2 cells were separately evaluated as described below. After additional incubation, the culture dishes were washed three times with fresh DMEM to remove the floating TiO_2 NPs, and finally the washed culture dishes were supplemented with 2 ml of fresh DMEM. The culture dish was placed on the transducer of the ultrasonic apparatus (Sonic Master ES-2, OG Giken Co., Ltd., Okayama, Japan) after the surface of the transducer was covered with 3 ml of water. Ultrasound was then irradiated from the bottom of the dishes under the following condition: frequency, 1 MHz; duty ratio, 50%; output power: 0.1 W/cm^2; and irradiation time, 30 s. After the TiO_2/US treatment, the dishes were incubated for 96 h. The culture medium was renewed at 48 h after the treatment. The viable cell number and apoptosis of HepG2 cells were evaluated at the prescribed time points.

2.4. TiO_2/US treatment in vivo

For the *in vivo* experiments using the mouse xenograft model, the HepG2 cells suspension in PBS (2×10^7 cells/ml) were mixed with one volume of Matrigel™ matrix (BD Bioscience, Franklin Lakes, NJ, USA), and the 0.1 ml aliquots were subcutaneously inoculated into the back of the BALB/c nude mice after being anesthetized with sodium pentobarbital (50 mg/kg, i.p.). When the tumor size reached an average diameter of 10–13 mm (about 2 weeks later), the *in vivo* experiments were started. The mice were randomly divided into three groups: (1) control group without treatment, (2) group with ultrasound irradiation, and (3) group with TiO_2/US treatment. Each group had six mice. After the mice were anesthetized with sodium pentobarbital (50 mg/kg, i.p.), 100 μl of the pre-S1/S2-GFP-TiO_2 NPs suspension (0.1% (w/v)) was directly injected into the tumor on the mice. The mice were then partially immersed into a water bath kept at 36 °C, and the tumor was exposed to the ultrasound using the ultrasonic apparatus (Sonic Master ES-2) under the following condition: frequency, 1 MHz; duty ratio, 50%; output power: 1 W/cm^2; and irradiation time, 60 s. The TiO_2/US treatment *in vivo* was repeated five times at days 0, 3, 6, 10 and 13, and the observation of mice was continued up to 28 days. The tumor volume was evaluated at the prescribed time points.

2.5. Evaluation for uptake of pre-S1/S2-immobilized TiO_2 NPs

The uptake of pre-S1/S2-GFP-TiO_2 NPs by HepG2 cells was evaluated by fluorescent immunocytochemistry for detecting the GFP tag on the TiO_2 NPs, according to the method described previously [27]. Anti-GFP mouse monoclonal antibody (Nakarai Tesqu, Kyoto, Japan) was used as the primary antibody, and Alexa Fluor 555 goat anti-mouse IgG antibody (Invitrogen, Carlsbad, CA, USA) and phycoerythrin-conjugated goat anti-mouse IgG antibody (Beckman Colter, Inc., Brea, CA, USA) were used as the secondary antibody for microscopy and flow cytometry, respectively. Observation of HepG2 cells was conducted using a fluorescent microscope (BZ-8000, KEYENCE, Osaka, Japan). For flow cytometry, the immunostained HepG2 cells were harvested by enzymatic treatment using a trypsin-EDTA solution (2.5 g/l trypsin (Sigma Aldrich, St. Louis, MO, USA) and 1 mM EDTA-2Na in PBS(−) buffer), and suspended in PBS(−) buffer. The fluorescent signal was detected using a flow cytometer (EPICS XL-MCL ADC, Beckman Colter, Inc., Brea, CA, USA).

2.6. Evaluation for OH radical generation

OH radical generation was evaluated by using aminophenyl fluorescein (APF, Sekisui Chemical Co., Ltd., Tokyo, Japan) which reacts with the OH radical to generate fluorescein. The TiO_2 NPs were added to the culture dishes containing 2 ml of 1 μM APF solution in PBS(−), in the absence of cells. The dish was then

irradiated with 1 MHz ultrasound at the intensities at 0–0.7 W/cm^2 for 30 s. The amount of fluorescein generated via the reaction of APF with OH radicals for 30 s was measured by a fluorescent plate reader (CytoFluor 4000, Applied Biosystems, Foster City, CA, USA) at an excitation and emission wavelength of 490 nm and 510 nm, respectively.

2.7. Evaluation for cell growth and apoptosis

Cell growth of the HepG2 were evaluated by counting the viable cells using a hemocytometer based on trypan blue exclusion, after harvesting cells by enzymatic treatment using a trypsin-EDTA solution.

Apoptosis of the HepG2 cells was evaluated based on three hallmarks, lowering of the mitochondrial membrane potential (hallmark for initiating phase of apoptosis), phosphatidylserine exposure on cell surface (for early phase of apoptosis), and nuclear chromatin condensation (for late phase of apoptosis) [33]. To detect the lowering of the mitochondrial membrane potential, HepG2 cells were stained with 5,5′,6,6′-tetrachloro-1,1′,3,3′-tetraethylbenzimidazolylcarbocyanine iodide (JC-1) using a JC-1 mitochondrial membrane potential assay kit (Cayman Chemical Company, Ann Arbor, MI, USA) per the manufacturer's instructions. In normal cells, JC-1 is incorporated into mitochondria, forming complexes with intense red fluorescence. In apoptotic cells with lower membrane potential, JC-1 remains in cytosol as the monomer, which shows green fluorescence. Red fluorescence from the JC-1 complex in mitochondria and green fluorescence from the JC-1 monomer in cytosol were observed using a fluorescent microscope (BZ-8000). To detect the phosphatidylserine externalization, HepG2 cells were stained with Annexin V using an Annexin V-FITC kit (Beckman Colter, Inc., Brea, CA, USA) because it has a high affinity for phosphatidylserine of cell membrane. Green fluorescence from fluorescein isothiocyanate (FITC) conjugated to Annexin V was observed using a fluorescent microscope. To detect the chromatin condensation, a DNA-specific fluorescent dye 4,6-diamino-2-phenylindole (DAPI) (Sigma) was used, which stains the condensed chromatin of apoptotic cells more brightly than the chromatin of normal cells. The culture dishes were washed twice with PBS(−) buffer, and the cells were immobilized with 500 μl of 4% (w/v) paraformaldehyde (PFA) solution for 30 min at room temperature (RT). After removal of the PFA solution, the cells were stained with 500 μl of 1 μg/ml DAPI solution for 30 min at RT. After washing three times with PBS(−) buffer, blue fluorescence from the DAPI-DNA complex was observed using a fluorescent microscope.

2.8. Evaluation of tumor volume

Tumor volume on the mouse xenograft model was evaluated according to the following equation. Tumor volume (mm^3) = 1/2 × (long diameter) × (short diameter)^2 [34], where long and short diameters of the tumors were measured with a slide caliper. Relative tumor volume was calculated as the ratio of the tumor volume to that before starting the TiO_2/US treatment.

2.9. Statistics

All data are presented as the means ± standard errors. Statistical analysis was performed using one-way analysis of variance (one-way ANOVA) followed by Bonferroni multiple-range test. The difference between the groups was considered to be significant when the p-value was less than 0.05.

3. Results

3.1. Uptake behavior of pre-S1/S2-immobilized TiO_2 NPs by HepG2 cells

To examine the kinetics of the pre-S1/S2 mediated uptake of TiO_2 NPs, the HepG2 cells were incubated with the pre-S1/S2-immobilized NPs for 0–24 h, and then the NPs bound to the cells was indirectly detected using GFP on the NPs as the molecular tag. Fig. 1 shows histograms of fluorescent intensity obtained from flow cytometry analysis. In the case of GFP-TiO_2 NPs (negative control), the histograms of the fluorescent signal from HepG2 cells were overlapped throughout the examined incubation time for uptake (Fig. 1A), indicating that the TiO_2 NPs without pre-S1/S2 were not incorporated by the HepG2 cells for 24 h. On the other hand, in the case of pre-S1/S2-GFP-TiO_2 NPs, the peak of the histogram was shifted to higher fluorescent intensity along with the incubation time up to 6 h, and saturated afterward (Fig. 1B). From these results, it was suggested that the incubation for 6 h was sufficient for the pre-S1/S2 mediated uptake of TiO_2 NPs by HepG2 cells.

Fig. 2 shows fluorescent images of immunostained HepG2 and WiDr cells after incubation with the TiO_2 NPs for 6 h. Uptake of the TiO_2 NPs by HepG2 cells was observed only when pre-S1/S2 was present on the NPs (Fig. 2A and B). Moreover, there was no uptake of pre-S1/S2-GFP-TiO_2 NPs by the human colon carcinoma WiDr (Fig. 2D), indicating the pre-S1/S2 mediated uptake of TiO_2

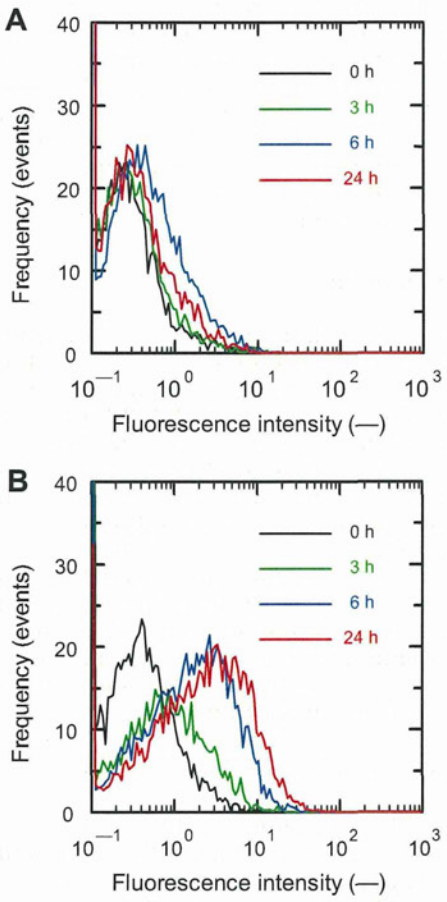

Fig. 1. Flow cytometry histograms of HepG2 cells after incubation with protein immobilized-TiO_2 NPs for 0–24 h. The uptake of GFP-TiO_2 NPs (A: negative control) and pre-S1/S2-GFP-TiO_2 NPs (B) was detected by immunostaining of HepG2 cells with anti-GFP monoclonal antibody.

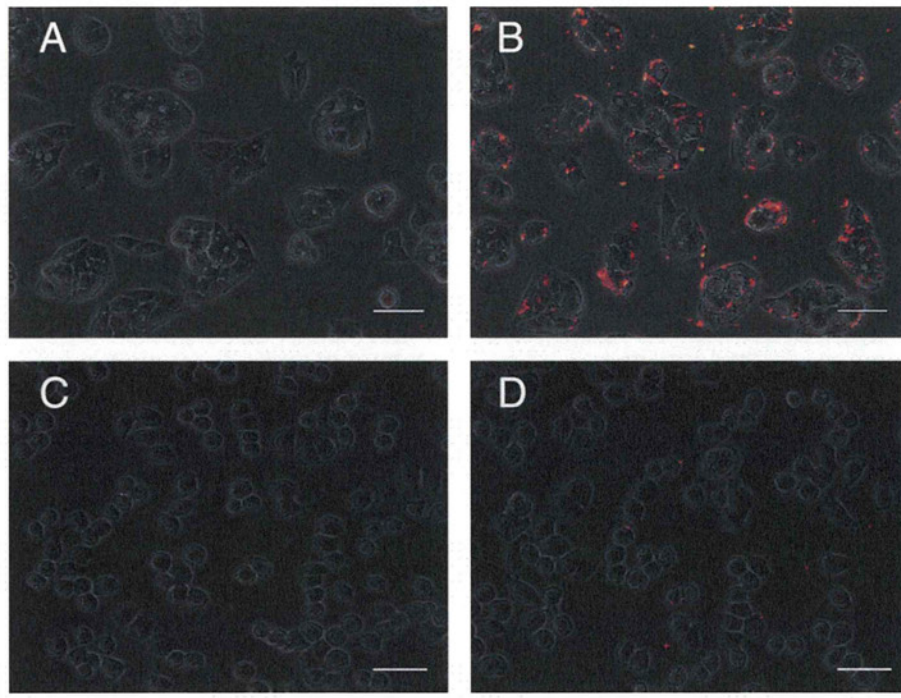

Fig. 2. Fluorescent microscopic images of HepG2 (A and B) and WiDr cells (C and D) after incubation with protein immobilized-TiO_2 NPs for 6 h. The uptake of GFP-TiO_2 NPs (A and C: negative control) and pre-S1/S2-GFP-TiO_2 NPs (B and D) was detected by immunostaining of cells with anti-GFP monoclonal antibody. Bars in the images indicate 50 μm.

NPs was specific to HepG2 cells. Therefore, these results validated the protein-immobilized TiO_2 NPs for targeted delivery toward the specific type of cells.

3.2. Effect of TiO_2/US treatment on growth and apoptosis of HepG2 cells

First, to examine the effect of ultrasound intensity on OH radical generation from TiO_2 NPs during the TiO_2/US treatment, ultrasound (0–0.7 W/cm^2) was irradiated to APF solution in the absence of cells. Fig. 3 shows the relationships between ultrasound intensity and fluorescent intensity derived from APF indicating OH radical generation. Although the OH radical was generated by the ultrasound irradiation itself, the presence of TiO_2 NPs enhanced the generation of the OH radical twice as the control, even at the lower intensity ultrasound at 0.1 W/cm^2. Therefore, ultrasound was irradiated at the intensity of 0.1 W/cm^2 in the following *in vitro* experiments.

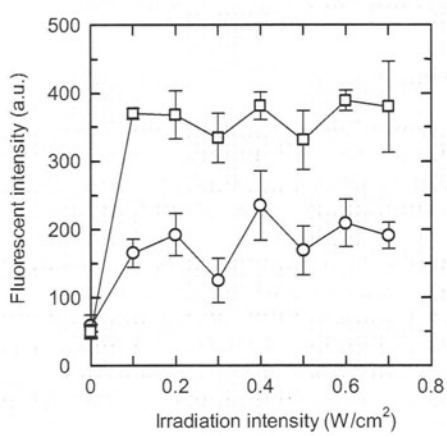

Fig. 3. Relationships between ultrasound irradiation intensity and fluorescent intensity derived from APF indicating the OH radical generated. Open circles: control with ultrasound irradiation only; open square: with addition of PAA-modified TiO_2 NPs and ultrasound irradiation. Data are the mean of three independent experiments, and the error bar indicates standard error.

Microscopic observation of HepG2 cells was conducted immediately after and at 48 h after the ultrasound irradiation to the cells with uptake of TiO_2 NPs for 6 h. Although no apparent cell damage was seen immediately after the TiO_2/US treatment (Fig. 4C), change in cellular morphology and reduction of cell number could be seen at 48 h after the TiO_2/US treatment (Fig. 4D). Therefore, to examine the effect of TiO_2/US treatment on the subsequent growth behavior of HepG2 cells, the cultures were traced for 96 h after the ultrasound irradiation to the cells with a 6 h uptake of the pre-S1/S2-GFP-TiO_2 NPs. Fig. 5 shows the time courses of viable cell numbers after the TiO_2/US treatment. In the control without treatment, the viable cell concentration increased with elapsed time, reaching 3.5×10^6 cells/ml at 96 h. In the case with ultrasound irradiation only, the growth profile was almost the same as the control condition, indicating that this low-intensity ultrasound itself had no influence on the HepG2 cell growth. Even in the case with the TiO_2/US treatment, there was no substantial decrease in viable cell numbers until 24 h compared with the other conditions. However, the cell growth rate was thereafter suppressed, and the viable cell concentration was 1.6×10^6 cells/ml at 96 h after the treatment (46% of the control). These results indicated that HepG2 cells were injured by the synergetic effect of the low-intensity ultrasound and the TiO_2 NPs incorporated to the cells. It was also indicated that the cell death was not apparent immediately after the treatment, but around 48 h after the treatment under the examined conditions.

To investigate the cell damage soon after the TiO_2/US treatment, apoptotic phenotype of the HepG2 cells was examined at 6 h after the TiO_2/US treatment. Fig. 6 shows the fluorescent images of HepG2 cells stained with JC-1, AnnexinV-FITC, and DAPI to detect

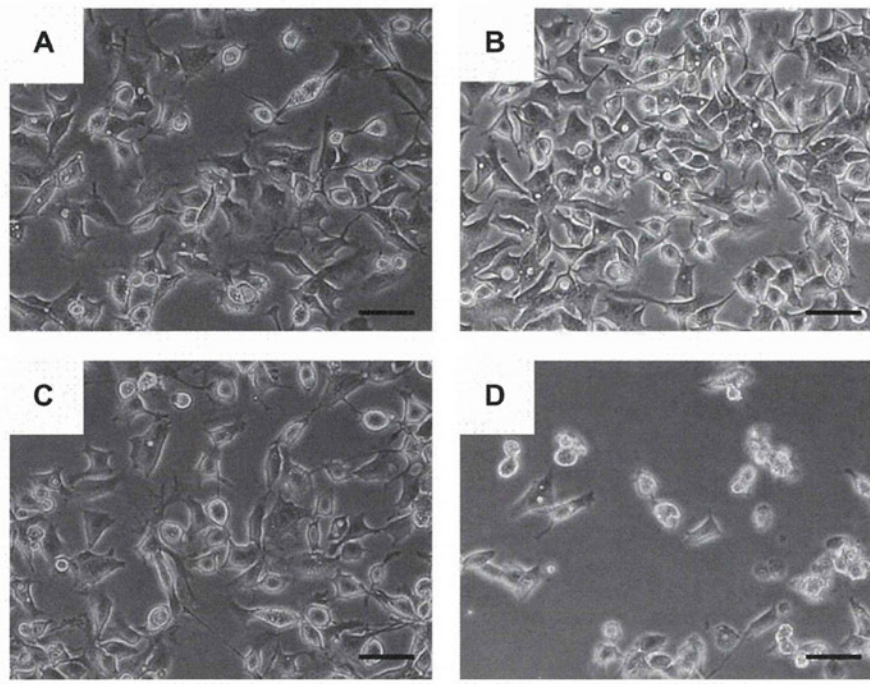

Fig. 4. Blight field microscopic images of HepG2 cells just after (A and C) and at 48 h after the treatment (B and D). (A and B) Control condition without treatment, (C and D) with TiO_2/US treatment. Each scale bar indicates 50 μm.

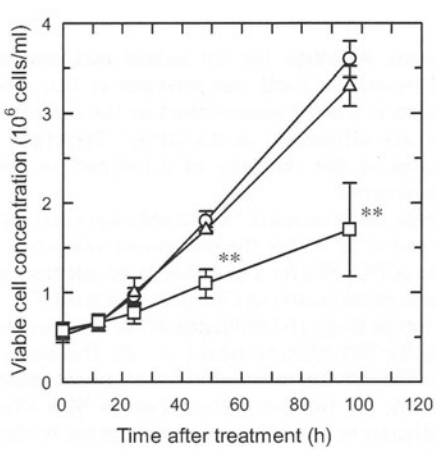

Fig. 5. Time courses of viable cell concentration of HepG2 after TiO_2/US treatment. Open circles: control condition without treatment; open triangles: with ultrasound irradiation only; open square: with TiO_2/US treatment. Data are the mean of four independent experiments, and the error bar indicates standard error. ** significantly different from the control groups ($p < 0.01$, one-way ANOVA followed by Bonferroni multiple-range test).

the lowering of the mitochondrial membrane potential (hallmark for initiating phase of apoptosis), phosphatidylserine exposure on cell surface (for early phase of apoptosis), and nuclear condensation (for late phase of apoptosis). In the case of the control without treatment, there was almost no apoptotic signal (Fig. 6A, C and E). However, in the case with the TiO_2/US treatment, the green fluorescence could be seen, indicating the loss of mitochondrial transmembrane potential (Fig. 6B) and phosphatidylserine exposure (Fig. 6D). Moreover, bright blue fluorescence derived from the condensed chromatin was also observed (Fig. 6F). From these observations, it was revealed that the TiO_2/US treatment induced the apoptosis of the HepG2 cells within 6 h after the treatment.

3.3. Anti-tumor effect of the TiO_2/US treatment

To examine the anti-tumor effect of the TiO_2/US treatment, the ultrasound was irradiated to the mouse xenograft model immediately after direct injection of pre-S1/S2-GFP-TiO_2 NPs to the tumor region. Fig. 7 shows the time courses of tumor growth on six mice in each group, where the TiO_2/US treatment was repeated five times within 13 days. In the group without treatment, the relative tumor volume in each mouse increased with elapsed time, reaching the range of 2.5–9.5 at 28 days. In the group with ultrasound irradiation only, the relative tumor volume exceeded 2.5 at 28 days in 5 mice out of 6 mice. In contrast, in the case with TiO_2/US treatment, the relative tumor volume of four mice became less than 2.5 at 28 days. These results suggested that the combination of the presence of TiO_2 NPs and ultrasound irradiation was effective in suppressing the tumor growth *in vivo*.

4. Discussion

Our previous study suggested the TiO_2/US treatment for cancer therapy, that is, SDT using the sonocatalyst TiO_2 NPs which was modified with targeting biomolecule [27]. The cell-injuring factors of the TiO_2/US treatment are considered to be roughly divided into the following: (1) Chemical factors such as the ROS generated due to the activation of TiO_2 under the ultrasound irradiation, which invites cell membrane oxidation. (2) Physical factors such as shear stress derived from the collapse of cavitation bubbles, which cause cell membrane disruption [4,26]. These chemical and physical factors observed under low-intensity ultrasound could trigger the apoptosis as well as invite the necrotic cell death mentioned above [35,36].

With regard to the chemical factor of the TiO_2/US treatment, the ROS can affect the cells more effectively when TiO_2 NPs are incorporated to the cells, since the ROS have very short half lives once they are generated on the surface of TiO_2. In this sense, it is a smart SDT strategy to modify the TiO_2 NPs with biomolecules specifically

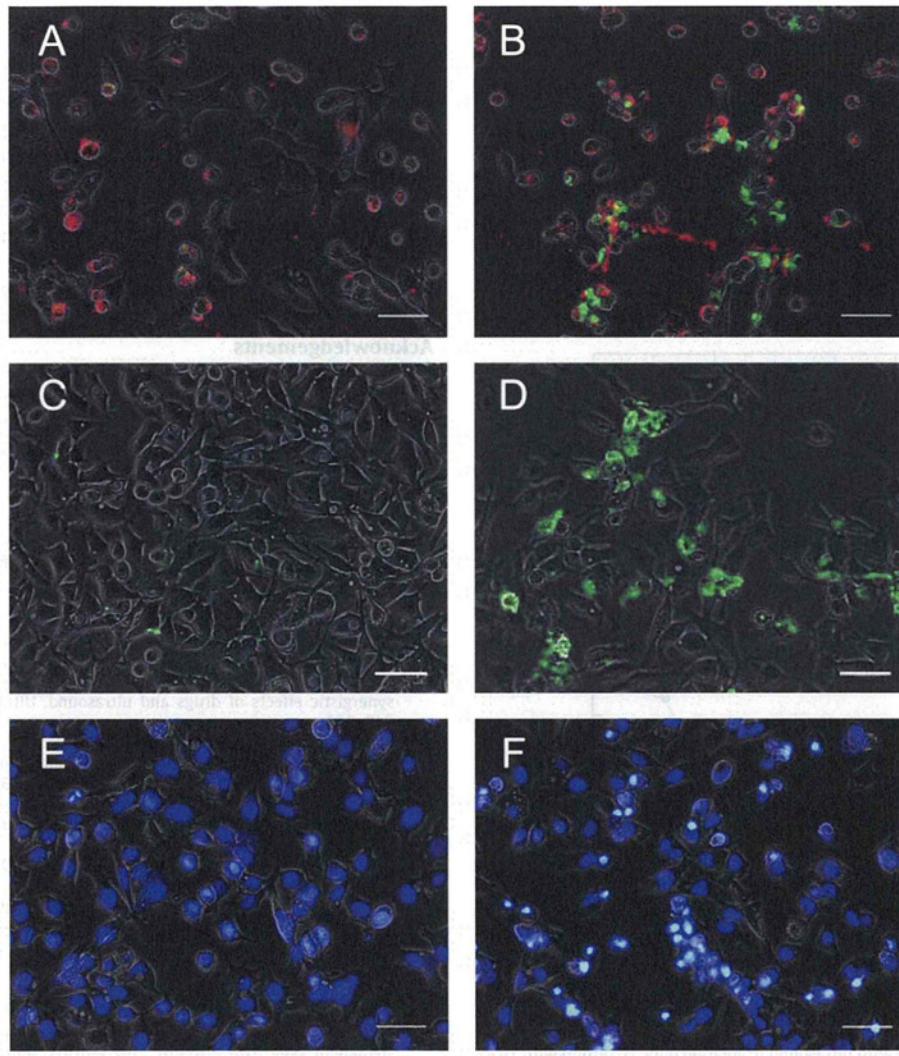

Fig. 6. Fluorescent microscopic images of HepG2 cells at 6 h after TiO_2/US treatment. The HepG2 cells were stained with JC-1 (A and B), Annexin V-FITC (C and D), and DAPI (E and F), respectively. (A, C and E) control condition without treatment, (B, D and F) with TiO_2/US treatment. The fluorescent images were merged with the phase-contrast ones. Each scale bar indicates 50 μm. (For interpretation of the references to colour in this figure legend, the reader is referred to the web version of this article.)

binding to target cells, as reported in the PDT using TiO_2 NPs [17–19]. The present study clarified that it took 6 h for the pre-S1/S2-mediated specific uptake of TiO_2 NPs by HepG2 cells (Fig. 1). This is consistent with the report that the fusion of the hepatitis B virus toward liver cells was complete within 6 h [30].

On the other hand, without pre-S1/S2, our TiO_2 NPs were not incorporated by either the HepG2 or WiDr cells under the examined condition (Fig. 2A and C). There is one report that the TiO_2 NPs used for the PDT was incorporated to glioma cells within 3 h, even without modification by any targeting biomolecules [15]. In general, the TiO_2 NPs which exhibit nonspecific incorporation cannot be used as a practical sonosensitizer for SDT, since it would also be accumulated to normal cells in the vicinity of the tumors and would react to ultrasound stimulus. Thus, it is important to prepare TiO_2 NPs, which are selectively accumulated to only target cancer cells.

Two other groups have applied the sonocatalytic effect of TiO_2 NPs to *in vitro* cancer cell injury [28,29]. In their reports, TiO_2 NPs were not modified with biomolecules for targeting specific cells. With regard to their ultrasonic conditions, 1 MHz ultrasound was irradiated for 10–50 s at the intensity of 1.0 W/cm^2, which was several times higher than in the present study. The cell viability was reduced to 50% of the control just after the TiO_2/US treatment, and was about 10% of the control at 24 h after the treatment. Yamaguchi et al. [28] revealed that cell injury by their TiO_2/US treatment was mainly attributed to physical factors such as shear stress (not to chemical factors such as ROS), judging from the experiment using glutathione as the radical scavenger. Thus it was supposed that in their TiO_2/US treatment condition, the membrane integrity of most cells was immediately disrupted by physical factors such as shear stress (namely, necrotic cell death), although a part of the treated cells exhibited the early-stage apoptotic phenotype at 24 h after the treatment.

On the other hand, in the present study employing the 1 MHz ultrasound for 30 s at 0.1 W/cm^2, the cell viability remained at 80–100% of the control until 24 h after the TiO_2/US treatment, and then dropped afterward (Fig. 5). In this sense, it was considered that the TiO_2/US treatment examined in this study did not induce necrotic cell death, but apoptotic cell death (Fig. 6) due to the physical (shear stress) and chemical factor (OH radical) generated by the combination of lower intensity ultrasound and TiO_2 NPs localized to the cells.

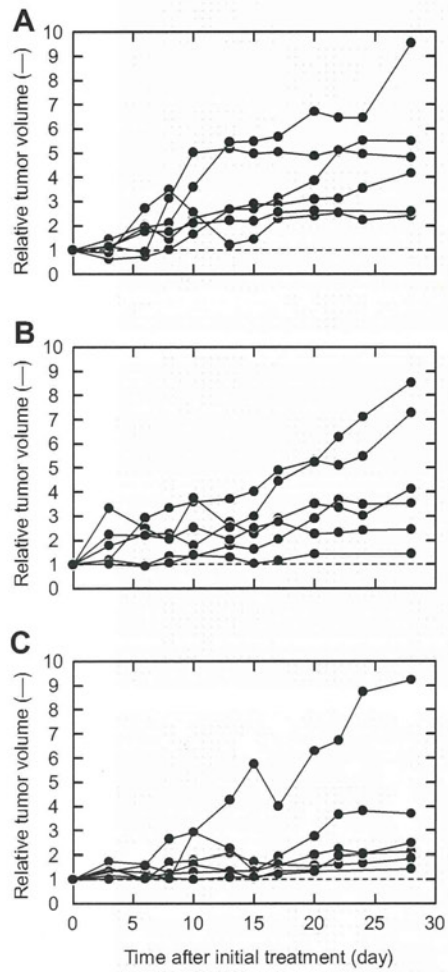

Fig. 7. Time courses of relative tumor volume on mouse xenograft model. TiO_2/US treatment was repeated five times at days 0, 3, 6, 10 and 13. (A) Control group without treatment; (B) group with ultrasound irradiation only; (C) group with TiO_2/US treatment. Each group had six mice. The dotted lines indicate unity of the relative tumor volume.

As for application of the sonocatalytic effect of TiO_2 NPs to *in vivo* cancer therapy, Harada et al. [29] first validated its practicability using a mouse xenograft model. In their study, 0.05 mg of TiO_2 NPs was injected directly into tumors, followed by 1 MHz ultrasound irradiation at 1.0 W/cm^2 for 120 s. Their TiO_2/US treatments were repeated five times during 8 days and resulted in the suppression of subsequent tumor growth compared with the control conditions, but could not achieve the regression of tumors within 21 days. In the present study, similar therapeutic results were obtained by the TiO_2/US treatment repeated five times during 13 days, by injecting 0.1 mg of pre-S1/S2-immobilized TiO_2 NPs and irradiating 1 MHz ultrasound at 1.0 W/cm^2 for 60 s (Fig. 7).

To enhance the anti-tumor effect of TiO_2/US treatment and realize complete regression, it might be necessary to accumulate much more TiO_2 NPs in the tumor regions. If TiO_2 NPs are injected via the tail vein, then many more targeting biomolecules should be immobilized on the NPs to improve the biodistribution of the NPs to tumors. With regard to ultrasound irradiation, it is better to employ the improved irradiation methodology for TiO_2/US treatment, such as the superimposition of dual ultrasounds [37,38], which can achieve a more efficient sonocatalytic reaction while maintaining the low-intensity of each ultrasound.

5. Conclusions

The availability of SDT using protein-immobilized TiO_2 NPs was examined *in vitro* and *in vivo*. The present study clarified the *in vitro* behavior of pre-S1/S2-mediated uptake of TiO_2 NPs by HepG2 cells. Moreover, this study also revealed the effect of TiO_2/US treatment on the immediate apoptosis induction and subsequent growth behavior of HepG2 cells. Finally, the TiO_2/US treatment could be applied to *in vivo* tumor therapy using a mouse xenograft model. For complete regression of tumors *in vivo*, further improvement of the TiO_2/US treatment is needed.

Acknowledgements

The present work was supported in part by a Grant-in-Aid for Scientific Research (B) (No. 19300182 to N.S.) from the Ministry of Education, Culture, Sports, Science and Technology, Japan.

References

[1] T.J. Mason, Therapeutic ultrasound an overview, Ultrason. Sonochem. 18 (2011) 847–852.
[2] J.E. Kennedy, High-intensity focused ultrasound in the treatment of solid tumours, Nat. Rev. Cancer 5 (2005) 321–327.
[3] T. Yu, Z. Wang, T.J. Mason, A review of research into the uses of low level ultrasound in cancer therapy, Ultrason. Sonochem. 11 (2004) 95–103.
[4] I. Rosenthal, J.Z. Sostaric, P. Riesz, Sonodynamic therapy–a review of the synergistic effects of drugs and ultrasound, Ultrason. Sonochem. 11 (2004) 349–363.
[5] M. Kuroki, K. Hachimine, H. Abe, H. Shibaguchi, S.I. Maekawa, J. Yanagisawa, T. Kinugasa, T. Tanaka, Y. Yamashita, Sonodynamic therapy of cancer using novel sonosensitizers, Anticancer Res. 27 (2007) 3673–3678.
[6] N. Yumita, R. Nishigaki, K. Umemura, Shin-ichiro umemura, hepatoporphyrin as a sensitizer of cell-damaging effect of ultrasound, Jpn. J. Cancer Res. 80 (1989) 219–222.
[7] T.J. Dougherty, J.E. Kaufman, A. Goldfarb, T.J. Dougherty, J.E. Kaufman, A. Goldfarb, K.R. Weishaupt, D. Boyle, A. Mittleman, Photoradiation therapy for the treatment of malignant tumors photoradiation therapy for the treatment of malignant tumors, Cancer Res. 38 (1978) 2628–2635.
[8] A. Fujishima, K. Honda, Electrochemical photolysis of water at a semiconductor electrode, Nature 238 (1972) 37–38.
[9] A. Fujishima, T.N. Rao, D.A. Tryk, Titanium dioxide photocatalysis, J. Photochem. Photobiol. C: Photochem. Rev. 1 (2000) 1–21.
[10] R. Cai, K. Hashimoto, I. Kiminori, Y. Kubota, A. Fujishima, Photokilling of malignant cells with ultrafine TiO_2 powder, Bull. Chem. Soc. Jpn. 64 (1991) 1268–1273.
[11] R. Cai, Y. Kubota, T. Shuin, R. Cai, Y. Kubota, T. Shuin, H. Sakai, K. Hashimoto, A. Fujishima, Induction of cytotoxicity by photoexcited TiO_2 particles advances in brief, Cancer Res. 52 (1992) 2346–2348.
[12] Y. Kubota, T. Shuin, C. Kawasaki, M. Hosaka, H. Kitamura, R. Cai, H. Sakai, K. Hashimoto, A. Fujishima, Photokilling of T-24 human bladder cancer cells with titanium dioxide, Br. J. Cancer 70 (1994) 1107–1111.
[13] A.-P. Zhang, Y.-P. Sun, Photocatalytic killing effect of TiO_2 nanoparticles on Ls-174-t human colon carcinoma cells, World J. Gastroenterol. 10 (2004) 3191–3193.
[14] J.-wook. Seo, H. Chung, M.-yun. Kim, J. Lee, I.-hong. Choi, J. Cheon, Development of water-soluble single-crystalline TiO2 nanoparticles for photocatalytic cancer-cell treatment, Small 3 (2007) 850–853.
[15] S. Yamaguchi, H. Kobayashi, T. Narita, K. Kanehira, S. Sonezaki, Y. Kubota, S. Terasaka, Y. Iwasaki, Novel photodynamic therapy using water-dispersed TiO_2-polyethylene glycol compound: evaluation of antitumor effect on glioma cells and spheroids *in vitro*, Photochem. Photobiol. 86 (2010) 964–971.
[16] C. Wang, S. Cao, X. Tie, B. Qiu, A. Wu, Z. Zheng, Induction of cytotoxicity by photoexcitation of TiO_2 can prolong survival in glioma-bearing mice, Mol. Biol. Rep. 38 (2011) 523–530.
[17] J. Xu, Y. Sun, J. Huang, C. Chen, G. Liu, Y. Jiang, Y. Zhao, Z. Jiang, Photokilling cancer cells using highly cell-specific antibody-TiO_2 bioconjugates and electroporation, Bioelectrochemistry 71 (2007) 217–222.
[18] E.A. Rozhkova, I. Ulasov, B. Lai, N.M. Dimitrijevic, M.S. Lesniak, T. Rajh, A high-performance nanobio photocatalyst for targeted brain cancer therapy, Nano Lett. 9 (2009) 3337–3342.
[19] K. Matsui, M. Karasaki, M. Segawa, S.Y. Hwang, T. Tanaka, C. Ogino, A. Kondo, Biofunctional TiO_2 nanoparticle-mediated photokilling of cancer cells using UV irradiation, Med. Chem. Commun. 1 (2010) 209–211.
[20] N. Shimizu, C. Ogino, M.F. Dadjour, K. Ninomiya, A. Fujihira, K. Sakiyama, Sonocatalytic facilitation of hydroxyl radical generation in the presence of TiO2, Ultrason. Sonochem. 15 (2008) 988–994.
[21] J. Wang, B. Guo, X. Zhang, Z. Zhang, J. Han, J. Wu, Sonocatalytic degradation of methyl orange in the presence of TiO_2 catalysts and catalytic activity comparison of rutile and anatase, Ultrason. Sonochem. 12 (2005) 331–337.

[22] N. Shimizu, C. Ogino, M.F. Dadjour, T. Murata, Sonocatalytic degradation of methylene blue with TiO_2 pellets in water, Ultrason. Sonochem. 14 (2007) 184–190.
[23] M. Stevenson, K. Bullock, W.-Y. Lin, K. Rajeshwar, Sonolytic enhancement of the bactericidal activity of irradiated titanium dioxide suspensions in water, Res. Chem. Intermed. 23 (1997) 311–322.
[24] M. Kubo, R. Onodera, N. Shibasaki-Kitakawa, K. Tsumoto, T. Yonemoto, Kinetics of ultrasonic disinfection of *Escherichia coli* in the presence of titanium dioxide particles, Biotechnol. Prog. 21 (2005) 897–901.
[25] M. Dadjour, C. Ogino, S. Matsumura, N. Shimizu, Kinetics of disinfection of by catalytic ultrasonic irradiation with TiO_2, Biochem. Eng. J. 25 (2005) 243–248.
[26] N. Shimizu, K. Ninomiya, C. Ogino, M.M. Rahman, Potential uses of titanium dioxide in conjunction with ultrasound for improved disinfection, Biochem. Eng. J. 48 (2010) 416–423.
[27] C. Ogino, N. Shibata, R. Sasai, K. Takaki, Y. Miyachi, Shun-ichi Kuroda, K. Ninomiya, N. Shimizu, Construction of protein-modified TiO_2 nanoparticles for use with ultrasound irradiation in a novel cell injuring method, Bioorg. Med. Chem. Lett. 20 (2010) 5320–5325.
[28] S. Yamaguchi, H. Kobayashi, T. Narita, K. Kanehira, S. Sonezaki, N. Kudo, Y. Kubota, S. Terasaka, K. Houkin, Sonodynamic therapy using water-dispersed TiO_2-polyethylene glycol compound on glioma cells: comparison of cytotoxic mechanism with photodynamic therapy, Ultrason. Sonochem. 18 (2011) 1197–1204.
[29] Y. Harada, K. Ogawa, Y. Irie, H. Endo, L.B. Feril, T. Uemura, K. Tachibana, Ultrasound activation of TiO_2 in melanoma tumors, J. Control. Release 149 (2011) 190–195.
[30] T. Yamada, Y. Iwasaki, H. Tada, H. Iwabuki, M.K.L. Chuah, T. VandenDriessche, H. Fukuda, A. Kondo, M. Ueda, M. Seno, K. Tanizawa, S. Kuroda, Nanoparticles for the delivery of genes and drugs to human hepatocytes, Nat. Biotechnol. 21 (2003) 885–890.
[31] T. Kasuya, T. Yamada, A. Uyeda, T. Matsuzaki, T. Okajima, K. Tatematsu, K. Tanizawa, S. Kuroda, In vivo protein delivery to human liver-derived cells using hepatitis B virus envelope pre-S region, J. Biosci. Bioeng. 106 (2008) 99–102.
[32] K. Kanehira, T. Banzai, C. Ogino, N. Shimizu, Y. Kubota, S. Sonezaki, Properties of TiO_2-polyacrylic acid dispersions with potential for molecular recognition, Colloids Surf. B. Biointerfaces 64 (2008) 10–15.
[33] D.R. Schultz, W.J. Harrington, Apoptosis: programmed cell death at a molecular level, Semin. Arth. Rheum. 32 (2003) 345–369.
[34] D.M. Euhus, C. Hudd, M.C. LaRegina, F.E. Johnson, Tumor measurement in the nude mouse, J. Surg. Oncol. 31 (1986) 229–234.
[35] L. Lagneaux, E.C. de Meulenaer, A. Delforge, M. Dejeneffe, M. Massy, C. Moerman, B. Hannecart, Y. Canivet, M.F. Lepeltier, D. Bron, Ultrasonic low-energy treatment: a novel approach to induce apoptosis in human leukemic cells, Exp. Hematol. 30 (2002) 1293–1301.
[36] L.B. Feril, T. Kondo, Z.-G. Cui, Y. Tabuchi, Q.-L. Zhao, H. Ando, T. Misaki, H. Yoshikawa, S. Umemura, Apoptosis induced by the sonomechanical effects of low intensity pulsed ultrasound in a human leukemia cell line, Cancer Lett. 221 (2005) 145–152.
[37] K. Kawabata, Effect of second-harmonic superimposition on efficient induction of sonochemical effect, Ultrason. Sonochem. 3 (1996) 1–5.
[38] S. Umemura, K. Kawabata, K. Sasaki, *In vitro* and *in vivo* enhancement of sonodynamically active cavitation by second-harmonic superimposition, J. Acoust. Soc. Am. 101 (1997) 569–577.

Journal of Drug Targeting, 2012; 20(10): 897–905

ISSN 1061-186X print/ISSN 1029-2330 online
DOI: 10.3109/1061186X.2012.725404

informa
healthcare

RESEARCH ARTICLE

Complex carriers of affibody-displaying bio-nanocapsules and composition-varied liposomes for HER2-expressing breast cancer cell-specific protein delivery

Yuya Nishimura[1], Jun Ishii[2], Fumiyoshi Okazaki[2], Chiaki Ogino[1], and Akihiko Kondo[1]

[1]*Department of Chemical Science and Engineering, Graduate School of Engineering, Kobe University, Nada, Kobe, Japan and* [2]*Organization of Advanced Science and Technology, Kobe University, Nada, Kobe, Japan*

Abstract

A bio-nanocapsule (BNC), a hollow particle composed of hepatitis B virus (HBV) surface antigen (HBsAg), and liposome (LP) conjugation method (BNC/LP) has been recently developed by Jung et al. (2008). The BNC/LP complex carrier could successfully deliver fluorescence-labeled beads (100 nm) into liver cells. In this study, we report the promising delivery of proteins incorporated in the complex carriers, which were prepared by the BNC/LP conjugation method with specificity-altered BNC and composition-varied LPs. The specificity-altered BNC, Z_{HER2}-BNC was developed by replacing the hepatocyte recognition site of BNC with Z_{HER2} binding to HER2 receptor specifically. Using green fluorescent protein (GFP; 27 kDa) and cellular cytotoxic protein (exotoxin A; 66 kDa) for the delivery, we herein present the impact of different charges attributed to the composition of the LP on specific cell targeting and cellular uptake of the complex carriers. In addition, we demonstrate that the mixture prepared by mixing LPs with helper lipid possessing endosomal escaping ability boosts the functional expression of the cellular cytotoxic exotoxin A activity specifically. Finally, we further show the blending ratio of the LP mixture and Z_{HER2}-BNC is a critical factor in determining the highly-efficient expression of the cytotoxic activity of exotoxin A.

Keyword: Controlled release, drug delivery, drug targeting, Hepatitis B virus, *in vitro* model, liposomes, nanoparticles

Abbreviations: DDS, drug delivery system; BNC, bio-nanocapsule; HBV, hepatitis B virus; HBsAg, hepatitis B virus surface antigen; HER2, human EGFR-related 2; EGFR, epidermal growth factor receptor; LP, liposome; GFP, green fluorescent protein; PEG, polyethylene glycol; CsCl, cesium chloride; DPPC, dipalmitoyl-phosphatidylcholine; CHOL, cholesterol; DPPG, dipalmitoyl-phosphatidylglycerol; DOPE, 1,2-dioleoyl-sn-glycero-3-phosphoethanolamine; DC6-14, O,O′-ditetradecanoyl-*N*-(α-trimethylammonioacetyl) diethanolamine chloride; FBS, Fetal bovine serum; DMEM, Dulbecco's modified Eagle medium; LSM, laser scanning microscope; EthD-1, ethidium homodimer-1; TLM, translocation motif

Introduction

A drug delivery system (DDS) is a technology that enables control of drug distributions in the body on the basis of quantitative, spatial and temporal aspects. If the delivery of biological active molecules (ex. DNA, RNA, medicinal chemicals and pharmaceutical proteins) universally becomes available, improvements in therapeutic effects and reductions in side effects should follow (Nagai, 2005; Tabata, 2006). The development of a variety of tools and carriers for DDS is an area of emerging research.

As the carrier, a bio-nanocapsule (BNC) that is composed of the L protein of the hepatitis B virus (HBV) surface antigen (HBsAg) and the lipid bilayer has many attractive features (Kuroda et al., 1992). The original BNC shows high specificity for human hepatocytes and high transfection efficiency equivalent to the original HBV. Moreover, BNC exhibits a reliable safety profile and can incorporate drugs and genes by an electroporation method since it is a viral-genome-free hollow nanoparticle (Yamada et al., 2003).

Address for Correspondence: A. Kondo, Department of Chemical Science and Engineering, Graduate School of Engineering, Kobe University, 1-1 Rokkodai, Nada, Kobe 657–8501, Japan. Tel.: +81 78 803 6196. Fax: +81 78 803 6196. E-mail: akondo@kobe-u.ac.jp
(Received 25 June 2012; revised 23 August 2012; accepted 27 August 2012)

Previously, we and other researchers succeeded in altering the cell-specificity of BNC by genetic modifications (Kasuya et al., 2008; Shishido et al., 2009a,b). Several varieties of specificity-altered BNCs could be generated by deleting the hepatocyte-specific recognition site (located in the preS region) in the L protein and inserting binding molecules with the ability to target other cells. Using this technique and an affibody molecule, a new class of affinity ligands derived from the Z domain of staphylococcal protein A (Orlova et al., 2006; Lee et al., 2008), we have constructed the Z_{HER2} affibody molecule displaying BNC on its surface (Z_{HER2}-BNC) whose specificity was successfully altered from hepatocytes to HER2 receptor expressing cells such as breast cancer and ovarian cancer cells (Shishido et al., 2010). In our previous study, we reported the specificity alteration of BNC by using the small and easily detectable molecule fluorescein, although further characterizations and applications of Z_{HER2}-BNC are still needed. For example, since the original HBV possesses the unique infectious entry mechanism of hepadnaviruses via receptor-mediated endocytosis followed by processing of a surface protein including the preS region in endosomes (Stoeckl et al., 2006), the specificity-altered Z_{HER2}-BNC in which the preS region is partly deleted, might result in the problematic trapping of medicinal agents within the endosomes.

Alternatively, a new method to conjugate BNCs with the liposome (LP) by first incorporating the materials together (BNC/LP conjugation method) was recently developed by Jung et al. (2008) as an alternative to the conventional electroporation method. They successfully demonstrated that the conjugated BNC/LP complex could incorporate large materials including fluorescence-labeled beads (100 nm). They also succeeded in delivering a GFP expression plasmid (>30 kbp) and specifically imparting green fluorescence to human hepatocytes both *ex vivo* and *in vivo* using the original BNC. This suggested that a new type of complex carrier based on the original BNC could release a gene into the cytoplasm by escaping from the endocytic pathway because of the unique endocytosis mechanism derived from original HBV (Jung et al., 2008). However, complex carriers prepared by conjugating the specificity-altered BNCs with LPs, in addition to preparation of complexes incorporating proteins that are comparatively large biomolecules have not been reported. Furthermore, the characteristics of LPs have not been reported as the features of the lipids used for the BNC/LP conjugation have never been evaluated closely.

In this study, we attempted for the first time to incorporate comparatively large proteins into the complex carriers prepared by the BNC/LP conjugation method with the specificity-altered BNC and also aimed to determine the impacts of characteristic lipids on the protein delivery. To confer the specificity for HER2-expressing cells on the complex carriers, we selected Z_{HER2}-BNC (Z_{HER2}-displaying BNC) for the conjugation with LPs. Moreover, we investigated the impact of LPs with different charges on the cell targeting specificities of the complexes and cellular uptake of the proteins when using three types of LPs, anionic-LP (ALP), nonionic-LP (NLP) and cationic-LP (CLP) for conjugating Z_{HER2}-BNC. Based on the obtained results, we investigated boosting the expression efficiency of the incorporated protein activity by using helper lipids with endosomal escaping abilities.

Material and methods

Materials

BNCs were prepared from *Saccharomyces cerevisiae* AH22R$^-$ harboring the plasmid pGLDsLd50-Z_{HER2} (Shishido et al., 2010) as described previously (Kuroda et al., 1992). Briefly, yeast cells transformed with pGLDsLd50-Z_{HER2} by the spheroplast method were cultured and disrupted with glass beads, the crude extract was precipitated with polyethylene glycol (PEG) 6000 and subjected to cesium chloride (CsCl) isopycnic ultracentrifugation and sucrose density gradient ultracentrifugation, and then the purified Z_{HER2}-BNC was obtained after freeze-drying in the presence of 5% sucrose. Green fluorescent protein (GFP) was obtained from One Shot® TOP10 Electrocomp™ *Escherichia coli* (Invitrogen Life Technologies, Carlsbad, CA, USA) harboring the plasmid to express the enhanced GFP containing His tag (pBAD, unpublished plasmid) by purifying the soluble fraction of the lysate using TALON metal affinity resins (Clontech Laboratories/Takara Bio, Shiga, Japan). Liposomes (LPs) were purchased from NOF (Tokyo, Japan). COATSOME EL-01-A [dipalmitoyl-phosphatidylcholine (DPPC): cholesterol (CHOL): dipalmitoyl-phosphatidylglycerol (DPPG) = 30: 40: 30 (μmol/vial)], COATSOME EL-01-N [DPPC: CHOL: DPPG = 54: 40: 6 (μmol/vial)] and COATSOME EL-01-C [DPPC: CHOL: stearyl-amine = 52: 40: 8 (μmol/vial)] were respectively selected as ALP, NLP and CLP. COATSOME EL-01-D [1,2-dioleoyl-*sn*-glycero-3-phosphoethanolamine (DOPE): CHOL: O,O′-ditetradecanoyl-*N*-(α-trimethylammonioacetyl) diethanolamine chloride (DC6-14) = 0.75: 0.75: 1.00 (μmol/vial)] was selected as the helper lipid. Pseudomonas exotoxin A from *Pseudomonas aeruginosa* was purchased from Sigma-Aldrich (St. Louis, MO, USA). Gibco® Fetal bovine serum (FBS), L-glutamine and Molecular Probes® LIVE/DEAD® viability/cytotoxicity assay kit were purchased from Invitrogen Life Technologies. RPMI 1640 medium and Dulbecco's modified Eagle medium (DMEM) were purchased from Nacalai Tesque (Kyoto, Japan). Leibovitz L-15 medium was purchased from MP Biomedicals (Irvine, CA, USA). Sephacryl™ S-500 HR column was purchased from GE Healthcare (Buckinghamshire, England).

Preparation of Z_{HER2}-BNC/ALP, NLP and CLP complexes incorporating GFP or exotoxin A

Complex carriers of Z_{HER2}-BNC and LPs (ALP, NLP and CLP), in which GFP or exotoxin A was incorporated, were prepared by referring to the previously described

BNC/LP conjugation method with some modifications (Jung et al., 2008). Freeze-dried LPs (COATSOME EL-01-A, 61 mg; EL-01-N, 61 mg; and EL-01-C, 57 mg) were dissolved in distilled water (2 mL) containing 2 mg/mL of GFP or 100 μg/mL of exotoxin A. After incubation for 1 h at room temperature, gel-filtration chromatography was performed only for the LPs containing GFP using a Sephacryl™ S-500 HR column with an AKTA system. The obtained LPs incorporating GFP or exotoxin A (100 μL) were added to freeze-dried Z_{HER2}-BNC (100 μg as protein) and incubated at room temperature for 1 h to form BNC/LP complexes incorporating GFP or exotoxin A. The resultant complex carriers were named Z_{HER2}-BNC/ALP, Z_{HER2}-BNC/NLP and Z_{HER2}-BNC/CLP.

Preparation of Z_{HER2}-BNC/DLP (DOPE-containing LP) complexes incorporating exotoxin A

Complex carriers of Z_{HER2}-BNC and DOPE-containing LP mixtures, in which exotoxin A was incorporated, were prepared according to the above-described method with the following modifications. To generate DOPE-containing LP mixtures (DLPs; ADLP or NDLP), 2.2 mg of COATSOME EL-01-A (ALP) or COATSOME EL-01-N (NLP) was added to 1 vial (1.5 mg) of COATSOME EL-01-D (DOPE-containing cationic helper lipid). By mixing various amounts of COATSOME EL-01-A (ALP) into a certain amount (1.5 mg) of COATSOME EL-01-D (DLP), the mixture ratio was determined to give the negative zeta potential (Supplementary Table S1). The generated LP mixture (ADLP or NDLP; 3.7 mg) was used as a substitute for the freeze-dried LPs in the previous section and dissolved in distilled water (1 mL). The amount of Z_{HER2}-BNC was varied from 0 to 100 μg (in terms of protein). The resultant complex carriers were named as Z_{HER2}-BNC/ADLP and Z_{HER2}-BNC/NDLP.

Cell culture

SKBR3 cells (human breast carcinoma, approximately 10^6 HER2 molecules expressed per cell (McLarty et al., 2009)) were maintained in RPMI 1640 medium supplemented with 10% (v/v) FBS at 37°C in 5% CO_2. MDA-MB-231 cells (human breast carcinoma) were maintained in Leibovitz L-15 medium supplemented with 15% FBS and 2 mM L-glutamine at 37°C without CO_2. HeLa cells (human cervical carcinoma) and MCF-7 cells (human breast carcinoma) were maintained in DMEM medium supplemented with 10% FBS at 37°C in 5% CO_2.

Microscopic observation of GFP delivery

Approximately 5×10^4 SKBR3 or MDA-MB-231 cells were seeded in 35 mm glass bottom dishes. After washing with serum-free medium, 20 μL of the complex carriers and LPs containing GFP were added to 980 μL of the medium and then the cells were cultured for 1 h. After washing with serum-free medium twice, cells were incubated with FBS-containing medium for 2 h. Cells were observed by a LSM 5 PASCAL laser scanning confocal microscope (Carl Zeiss, Oberkochen, Germany) using a 63-fold oil immersion objective lens with excitation using the 488-nm line of an argon laser and emission collection using a 505-nm long pass filter.

Microscopic observation of exotoxin A delivery

Approximately 2×10^5 SKBR3, MCF-7 or HeLa cells were seeded in 12-well plates. After washing with serum-free medium, the required volumes of the complex carriers and LPs containing exotoxin A were added to the medium and the volume was adjusted to 1 mL and then cells were cultured for 1 h. After washing with serum-free medium twice, the cells were incubated with FBS-containing medium for 47 h. Dead cells were stained with ethidium homodimer-1 (EthD-1) from the LIVE/DEAD® viability/cytotoxicity assay kit according to the manufacturer's instructions. Cells were observed by laser scanning confocal microscope using the same procedure described in the previous section except for employing excitation using the 543-nm line of an He-Ne laser and emission collection using a 560-nm long pass filter.

Flow cytometric evaluation of exotoxin A delivery

The cells were treated with the complex carriers and LPs containing exotoxin A in the same manner as described in the previous section. Live cells were stained with calcein AM from the LIVE/DEAD® viability/cytotoxicity assay kit according to the manufacturer's instructions. Cells were suspended into sheath solution and subjected to a BD FACSCanto II flow cytometer equipped with a 488-nm blue laser (BD Biosciences, San Jose, CA, USA). The green fluorescence signals were collected through a 530/30-nm band-pass filter. The data were analyzed using the BD FACSDiva software v5.0 (BD Biosciences). Dead cell numbers were estimated by subtracting the viable cell counts from total cell counts.

Measuring the sizes and zeta potentials of particles

The sizes and zeta potentials of the LPs and BNC-LP complexes were determined by a Zetasizer Nano ZS (Malvern Instruments, Worcestershire, UK), following the manufacturer's procedure.

Results and discussion

The main purpose of this study was to investigate how cancer cell-specific drug delivery is affected by the type of LP which is used to prepare the complex carriers that incorporate the medicinal agents by the BNC/LP conjugation method (Jung et al., 2008). Additionally, we also investigated target-cell-specific protein delivery since there have been no reports regarding complex carriers using specificity-altered BNCs and the incorporation of proteins. By conjugating various kinds of LPs with Z_{HER2}-displaying BNC (Z_{HER2}-BNC) in which the hepatocyte-specific recognition site of original BNC was genetically altered to the HER2-specific binding molecule Z_{HER2} (Shishido et al., 2010), we evaluated the specificity of the complexes to target HER2-expressing

SKBR3 breast cancer cells and the expression efficiency of the incorporated protein activity. At the same time, we used three types of HER2-negative cells (MDA-MB-231, HeLa and MCF-7) to show clearly HER2-specific binding ability of the complexes. First, we visually observed the targeting specificities and cellular uptakes of the BNC/LP complexes incorporating the fluorescent protein GFP (27 kDa). Subsequently, we examined the expression efficiencies of cell cytotoxicity with the variety of composition-altered BNC/LP complexes, which incorporate the cytotoxic protein, *Pseudomonas* exotoxin A (66 kDa), that can kill cells by inhibiting protein synthesis via the ADP ribosylation of elongation factor 2 (Allured et al., 1986).

Influence of different charges of LPs with varied lipid compositions on cell targeting specificities and cellular uptakes of Z_{HER2}-displaying BNC/LP complexes

To examine the influence of different charges of LPs with varied lipid compositions on the cell targeting specificities and cellular uptakes of Z_{HER2}-displaying BNC/LP complexes, we conjugated Z_{HER2}-BNC with three kinds of LPs: ALP, NLP and CLP (COATSOME EL-01-A, EL-01-N and EL-01-C), respectively. The resultant complex carriers were named Z_{HER2}-BNC/ALP, Z_{HER2}-BNC/NLP and Z_{HER2}-BNC/CLP. Through the conjugations, GFP was incorporated into each Z_{HER2}-BNC/LP complex so that its cellular localization could be visualized. All three types of LPs incorporating GFP without the conjugation to the Z_{HER2}-BNC were also used for comparison purposes. After 1 h of incubation with the LPs or the Z_{HER2}-BNC/LP complexes, HER2-positive SKBR3 cells (Davison et al., 2011) and HER2-negative MDA-MB-231 cells (Davison et al., 2011) were washed twice and additionally incubated for 2 h, and then observed by the confocal laser scanning microscope (Figure 1).

Both types of cells treated with the ALP and the NLP lacking the Z_{HER2}-BNC conjugations did not show fluorescence (Figure 1). MDA-MB-231 cells also exhibited no fluorescence after treatment with the Z_{HER2}-BNC/ALP and Z_{HER2}-BNC/NLP complexes, whereas after treatment, SKBR3 cells exhibited the green fluorescence inside the cells (Figure 1). These results indicate that the LPs with an anionic or nonionic charge could obtain the HER2-specific targeting ability by conjugation with the Z_{HER2}-displaying BNC, thereby permitting cellular uptake of the BNC/LP complexes incorporating GFP.

Both SKBR3 and MDA-MB-231 cells treated with the CLP and the Z_{HER2}-BNC/CLP complex showed green fluorescence on the periphery of the cell membranes (Figure 1). Due to the cationic charge of CLP, it would be presumed that even the conjugated complex with Z_{HER2}-BNC has non-specifically bound to the negatively-charged cell membrane through electrostatic interactions. Indeed, the Z_{HER2}-BNC/CLP complex showed the positively-charged zeta potential (Supplementary Table S2). These results suggest that the LPs with anionic or nonionic charges are favorable for the preparation of the BNC/LP complex by conjugation because the cell targeting specificity of BNC can be maintained.

Incorporation of cytotoxic protein, exotoxin A, into Z_{HER2}-displaying BNC/LP complexes prepared by using LPs with different charges

To investigate whether the Z_{HER2}-BNC/LP complexes prepared by using the LPs with different charges are able to express the incorporated protein activity in keeping with the specificity towards HER2-expressing target cells, we prepared the LPs and Z_{HER2}-BNC/LP complexes incorporating the cell cytotoxic exotoxin A with ALP, NLP and CLP. After 1 h of incubation with the obtained LPs or Z_{HER2}-BNC/LP complexes, HER2-positive SKBR3 cells and HER2-negative MCF-7 cells (Davison et al., 2011) were washed twice and additionally incubated for 47 h, and then stained with EthD-1, which displays red fluorescence via a dead-cell-specific uptake mechanism. Then, the stained cells were observed by confocal laser scanning microscopy to check the expression of cell-killing activity resulting from the effectiveness of exotoxin A (Figure 2).

Both the SKBR3 (target cells) and MCF-7 (control cells) treated with the CLP and Z_{HER2}-BNC/CLP complexes incorporating exotoxin A exhibited red fluorescence, showing that both carriers non-specifically caused cell death regardless of whether or not the cells were expressing the HER2 receptor (Figure 2). It is thought that the carriers containing the LPs with cationic charges bound to the cell surface in a non-specific fashion and then released the exotoxin A into the cytoplasm by membrane fusion in both target and non-target cells.

Both cells treated with the Z_{HER2}-BNC/ALP and Z_{HER2}-BNC/NLP complexes never displayed red fluorescence (Figure 2). As expected, both cells treated with the ALP and NLP lacking the Z_{HER2}-BNC also showed nearly no fluorescence (Figure 2). These results indicated that the Z_{HER2}-BNC/LP complexes composed of the LPs with anionic and nonionic charges did not lead to the death of MCF-7 control cells or SKBR3 target cells since they were probably unable to effectively express the cytotoxic activity of exotoxin A inside the cells. This was also supported by the results of quantitative FACS analysis used to measure the fatality rates of target cells (SKBR3) and non-target cells (HeLa) (Jia et al., 2003) with the same complexes containing exotoxin A (Figure 3A and 3B; white bars). Because SKBR3 cells treated with the Z_{HER2}-dispalying BNC/LP complexes incorporating GFP by the conjugation with ALP and NLP showed locally punctate fluorescence patterns (Figure 1), it was expected that the exotoxin A would be introduced into HER2-expressing SKBR3 cells via receptor-mediated endocytosis but remain within the endosome without being released into cytoplasm, resulting in no expression of cell-killing activity. This seemed to be different from the result obtained for the plasmid incorporated complex carrier prepared by using the original BNC (Jung et al., 2008). Previously it had been elucidated that the endosomal escape of

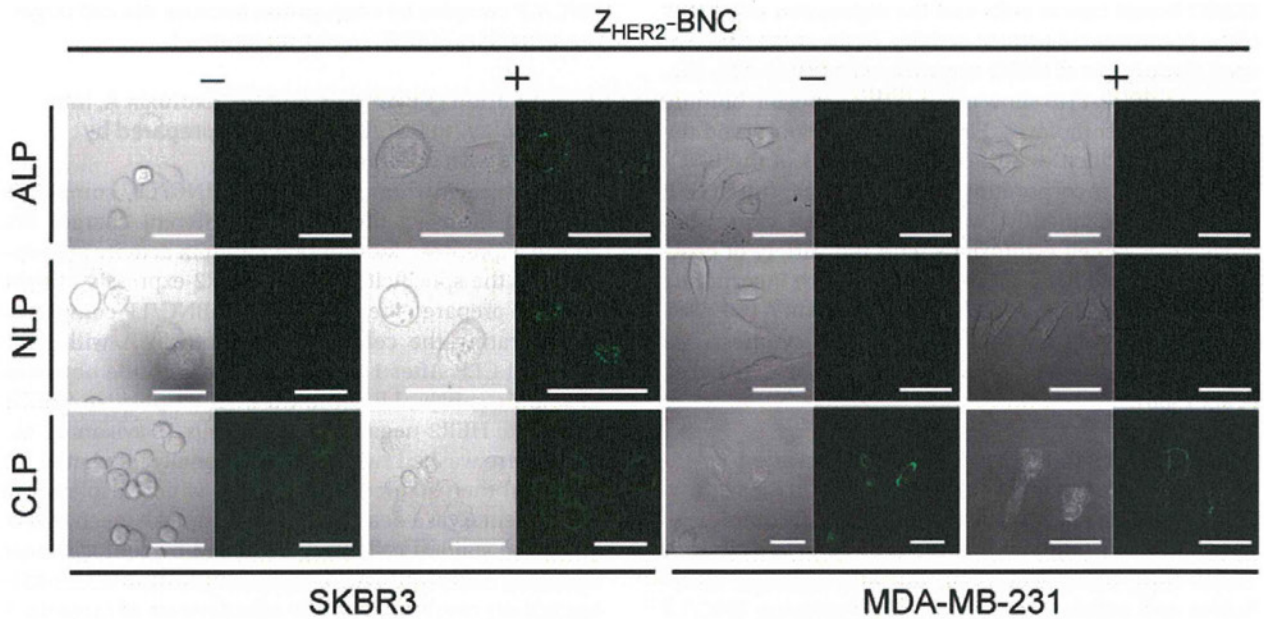

Figure 1. Fluorescence images of HER2-positive SKBR3 and HER2-negative MDA-MB-231 cells treated with ZHER2-BNC/LP complexes incorporating GFP. ALP, NLP and CLP with different (anionic, nonionic and cationic) charges were dissolved in distilled water containing 2 mg/mL of GFP, and then were used to prepare the ZHER2-BNC/LP complexes as described in "Materials and methods". All three types of LPs incorporating GFP without conjugation to the ZHER2-BNC were also used as the carriers for comparison. Cells were incubated for 1 h in the media adjusted to 1 mL by adding 20 μL of the complex carriers and LPs, respectively. After washing twice, cells were additionally incubated for 2 h and then observed by a confocal laser scanning microscope. Scale bar, 50 μm.

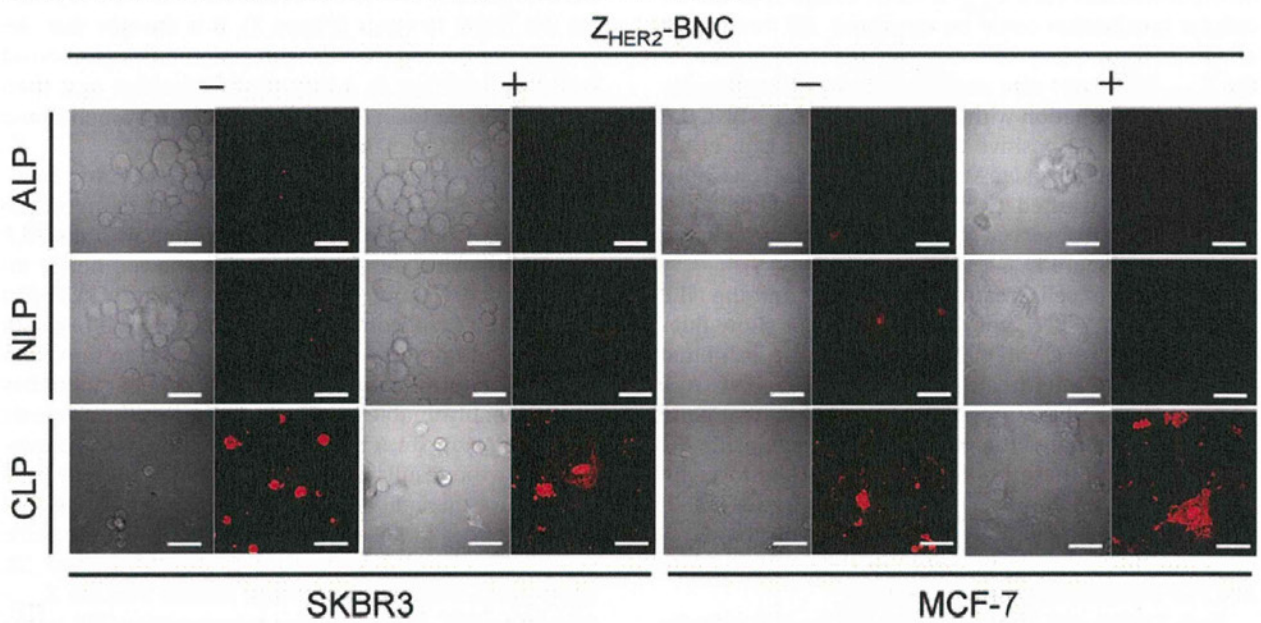

Figure 2. Fluorescence images of HER2-positive SKBR3 and HER2-negative MCF-7 cells treated with ZHER2-BNC/LP complexes incorporating exotoxin A. ALP, NLP and CLP with different (anionic, nonionic and cationic) charges were dissolved in distilled water containing 100 μg/mL of exotoxin A, and then were used to prepare the ZHER2-BNC/LP complexes as described in "Materials and methods". All three types of LPs incorporating exotoxin A without conjugation to the ZHER2-BNC were also used as the carriers for comparison. Cells were incubated for 1 h in the media adjusted to 1 mL by adding 20 μL of the complex carriers and LPs, respectively. After washing twice, cells were additionally incubated for 47 h and then stained with EthD-1. Then, the stained cells were observed by a confocal laser scanning microscope. Scale bar, 50 μm.

original HBV is induced by the unmasked cell-permeable peptide [translocation motif (TLM); located in the preS region] that is exposed on the surface of mature viral particles across the conformational changes in surface proteins arising from processing by endosomal proteases (Stoeckl et al., 2006). However, since the TLM sequence was deleted when constructing the Z_{HER2}-BNC with the aim to minimize the preS region in order to reduce the

antigenic region and the possibility of protease degradation (Shishido et al., 2009a,b), the unique endocytosis mechanism of the original BNC might be attenuated (Oess & Hildt, 2000).

These results suggest that the target-cell-specific expression of the cell-killing activity of exotoxin A with the Z_{HER2}-displaying BNC/LP complex containing ALP or NLP requires a mechanism to release the incorporated proteins from the endosome into the cytoplasm.

Expression of exotoxin A activity specifically in HER2-expressing cells with Z_{HER2}-BNC/LP complex prepared by mixing helper lipid

In order to improve the ability of the Z_{HER2}-BNC/ALP or Z_{HER2}-BNC/NLP complex to escape the endosome, we conceived the use of a helper lipid. We chose a pH-sensitive DOPE contained CLP (COATSOME EL-01-D) as the helper lipid to assist the escape from the endosome through the destabilization of the endosomal membrane via a conformational change in acidic conditions. We incorporated exotoxin A into the LP mixtures which were prepared by mixing the DOPE contained CLP with the anionic and nonionic ALP and NLP, respectively. The obtained LP mixtures (ADLP and NDLP) were conjugated with Z_{HER2}-BNC to produce the DOPE and exotoxin A contained complex carriers (Z_{HER2}-BNC/ADLP and Z_{HER2}-BNC/NDLP). After 1 h of incubation with the various amounts of Z_{HER2}-BNC/ADLP and Z_{HER2}-BNC/NDLP complexes containing exotoxin A, HER2-positive SKBR3 cells and HER2-negative HeLa cells were washed twice and incubated for an additional 47 h, and then stained with calcein AM, which displays green fluorescence via live-cell-specific uptake. Then the fatality rates of the cells were measured by subtracting the live-cell-counts from the total-cell-counts obtained from the quantitative FACS analysis (Figure 3A and 3B; gray bars).

HER2-positive SKBR3 target cells added to more than 20 μL of the DOPE-containing Z_{HER2}-BNC/ADLP complex (Figure 3A; gray bars) showed higher fatality rates than the DOPE-free Z_{HER2}-BNC/ALP (Figure 3A; white bars). As the addition of 50 μL of the Z_{HER2}-BNC/ADLP complex rarely led to the death of non-target cells (HeLa; Figure 3A), it confirmed that displaying Z_{HER2} on the BNC/ADLP complex functionally provided the HER2-positive SKBR3-specific cytotoxic effect. These results suggest that the DOPE-containing LP in the Z_{HER2}-BNC/ADLP complex successfully functioned as a helper lipid to assist the endosomal escape and express the cell cytotoxic activity of the incorporated exotoxin A, although the fatality rates of SKBR3 cells were still not very high.

The DOPE and exotoxin A contained Z_{HER2}-BNC/NDLP complex produced high fatality rates in target SKBR3 cells (Figure 3B; gray bars). However, the complex also produced a high fatality rate even in non-target HeLa cells (Figure 3B; HeLa, gray bar). The Z_{HER2}-BNC/NDLP complex, which was prepared with the mixture of the nonionic LP (NLP) and the DOPE contained CLP was introduced into both target and non-target cells non-specifically

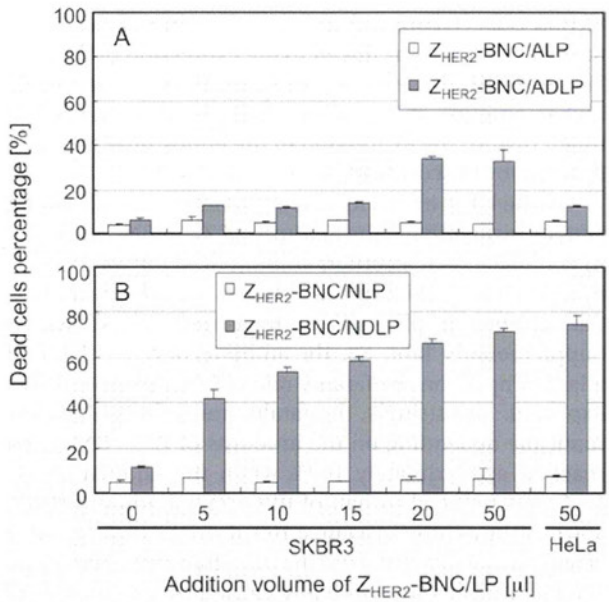

Figure 3. Fatality rates of HER2-positive SKBR3 and HER2-negative HeLa cells treated by the exotoxin A containing ZHER2-BNC/LP complexes with and without helper lipid. DOPE-containing cationic LP was selected as the helper lipid and mixed with ALP or NLP to generate DOPE-containing LP mixtures (ADLP or NDLP). The LP mixtures (ADLP or NDLP) or LPs (ALP or NLP) were dissolved in distilled water containing 100 μg/mL of exotoxin A, and then used to prepare the ZHER2-BNC/LP complexes as described in "Materials and methods". Cells were incubated for 1 h in the media adjusted to 1 mL by adding the indicated volumes of the complex carriers. After washing twice, cells were additionally incubated for 47 h and then stained with calcein AM. Then, the stained cells were analyzed using a flow cytometer. Dead cell numbers were estimated by subtracting the viable cell counts from total cell counts.

perhaps because of a shift of surface charge in the complex to cationic. Indeed, the zeta potential was a negative value for the Z_{HER2}-BNC/ADLP complex and a positive value for the Z_{HER2}-BNC/NDLP complex (Supplementary Table S2). The LP mixtures (ADLP and NDLP) also showed the same tendencies (Supplementary Table S2). In addition, the sizes of Z_{HER2}-BNC/ADLP and Z_{HER2}-BNC/NDLP complexes were almost unchanged (Supplementary Table S2). These results demonstrated that the conjugation of Z_{HER2}-displaying BNC with the LP mixture (ADLP) obtained by mixing the ALP (COATSOME EL-01-A) and the DOPE-containing CLP (COATSOME EL-01-D) could functionally confer the ability to enable the endosomal escape of the incorporated protein as well as the ability to specifically target the HER2-expressing cells.

Effective expression of exotoxin A activity using the complex carrier with the optimized blended ratio of Z_{HER2}-BNC and DOPE-containing anionic LP mixture (ADLP)

Next, we considered an approach to enrich the expression efficiency of the cytotoxic effect of the Z_{HER2}-BNC/ADLP complex incorporating exotoxin A. We assumed that the reason for the low fatality rates of the target

SKBR3 cells (Figure 3A) was that the ratio of the ADLP to the Z_{HER2}-BNC was linked to the expression of the cell-killing activity of the incorporated exotoxin A. A relatively higher amount of Z_{HER2}-BNC conjugated to the ADLP might disturb the expression of the endosomal escaping function by obscuring the efficacy of DOPE.

On the basis of this idea, we examined the cell-killing activity by modifying the amounts of Z_{HER2}-BNC available to conjugate with a certain amount of ADLP incorporating exotoxin A (Figure 4A). The sizes and zeta potentials of the complexes were measured and shown in Supplementary Table S3. The amounts of Z_{HER2}-BNC had a large impact on the fatality rates of SKBR3 cells as was expected. Surprisingly, the fatality rates fluctuated dramatically depending on the amounts of Z_{HER2}-BNC, and reached approximately 100% when the additive Z_{HER2}-BNC was reduced to half of the original amount (from 100 to 50 μg as protein against 100 μL-ADLP (3.7 mg/mL)) (Figure 4A). It was inferred that the dramatic decrease of the fatality rates was probably caused by attenuation of the HER2-specific binding ability when the amount of additive Z_{HER2}-BNC was reduced to less than 1/3. When the Z_{HER2}-BNC-halved complex was added to SKBR3 and HeLa, cell death was specific to only the target SKBR3 cells (Figure 4B). The anionic LP mixture (ADLP) containing exotoxin A never showed the cell-killing activity in both cells (Figure 4B). These results indicated that we could express the function of the incorporated protein into the Z_{HER2}-BNC/ADLP complex by determining the optimized blending ratio of Z_{HER2}-BNC and anionic LP mixture [Z_{HER2}-BNC: ADLP = 50 μg as protein: 100 μL (3.7 mg/mL)]. Thus, we succeeded in developing the specificity-altered BNC/LP complex containing the bifunctional properties of cell-specificity and endosomal escape.

Evaluation of cell-killing activity when adding various amounts of the optimized blended Z_{HER2}-BNC/ADLP complexes containing exotoxin A

Finally, we evaluated the cell-killing activities when adding various amounts of the optimized blended complexes containing exotoxin A (Figure 5). Even when adding 5 μL of the optimized blended Z_{HER2}-BNC/ADLP complex, the fatality rate of SKBR3 cells was over 50%. The fatality rates were enriched in a dose-dependent manner, producing approximately 100% cell death when 20 μL of the complex was added. The ADLP lacking Z_{HER2}-BNC containing exotoxin A could not kill the SKBR3 cells efficiently despite increasing the addition volume up to 50 μL. Direct addition of 50 μL of exotoxin A (100 μg/mL) without any carriers also never produced the death of SKBR3 cells. These results indicate that cellular uptake and release into the cytoplasm of exotoxin A were surely attributed to the Z_{HER2}-BNC/ADLP complex carrier. In addition, the Z_{HER2}-BNC/ADLP complex without exotoxin A rarely affected the fatality rate of SKBR3 cells, suggesting that the complex itself displayed low cellular toxicity. Furthermore, high specificity to HER2-expressing cells was exhibited

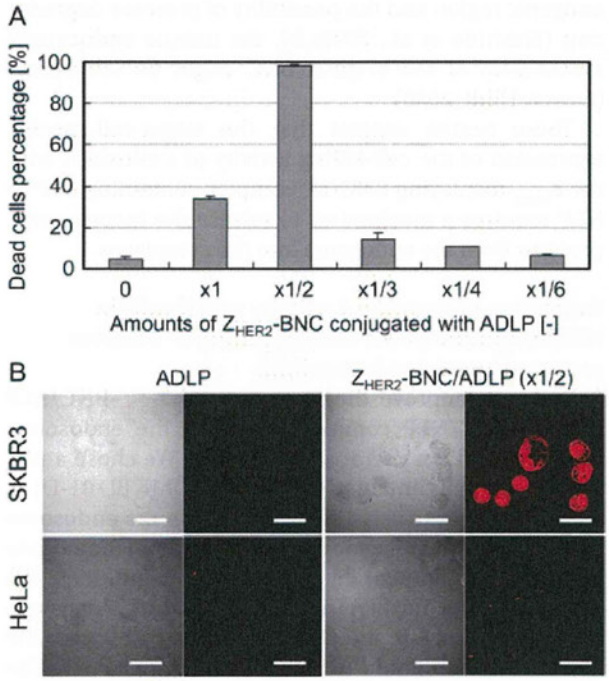

Figure 4. Modification of the amounts of ZHER2-BNC for conjugation with the DOPE contained LP mixture (ADLP). The LP mixture was dissolved in distilled water containing 100 μg/mL of exotoxin A, and then used to prepare the complex carriers with varied amounts of ZHER2-BNC as described in "Materials and methods". Cells were incubated for 1 h in the media adjusted to 1 mL by adding the indicated volumes of the complex carriers. After washing twice, cells were additionally incubated for 47 h. (A) Fatality rates of HER2-positive SKBR3 cells treated with the complex carriers containing varied amounts of ZHER2-BNC. The abscissa axis shows relative amounts of the added ZHER2-BNC against 100 μl-ADLP (3.7 mg/mL); For 0, x1, x1/2, x1/3, x1/4 and x1/6, 0, 100, 50, 33, 25 and 16 μg of ZHER2-BNC (as protein) were used, respectively. Cells were stained with calcein AM and then analyzed using a flow cytometer. Dead cell numbers were estimated by subtracting the viable cell counts from total cell counts. (B) Fluorescence images of HER2-positive SKBR3 and HER2-negative HeLa cells treated with LP mixture (ADLP) or the optimized blended ZHER2-BNC/ADLP complex (x1/2). Cells were stained with EthD-1 and then observed by a confocal laser scanning microscope. Scale bar, 50 μm.

by the low fatality rate of non-target HeLa cells even when adding 50 μL of the Z_{HER2}-BNC/ADLP complex. The complex carrier prepared with the BNC displaying wild-type Z domain (Z_{WT}-BNC/ADLP) never exhibited cellular toxicity to HER2-expressing SKBR3 cells (Supplementary Figure S1). These results successfully demonstrate that the optimized blended Z_{HER2}-BNC/ADLP complex could be a potential carrier to provide protein therapy for HER2 positive breast cancer cells.

Conclusions

As previously reported, the results presented herein confirm the HER2-specific targeting ability of Z_{HER2}-BNC. However, the delivery capacity of Z_{HER2}-BNC for protein therapy has remained obscure. We report here the design

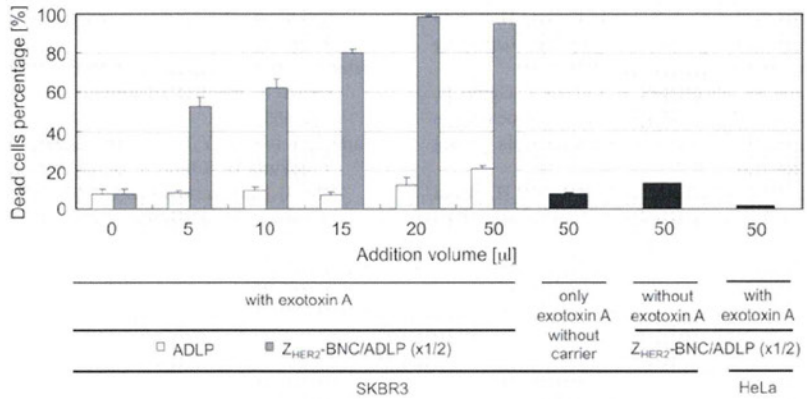

Figure 5. Fatality rates of HER2-positive SKBR3 and HER2-negative HeLa cells treated by the indicated carriers with and without exotoxin A. The DOPE-containing LP mixture (ADLP) was dissolved in distilled water containing 100 μg/mL of exotoxin A, and then was used to prepare the optimized blended ZHER2-BNC/ADLP complex shown in Figure 4. Cells were incubated for 1 h in the media adjusted to 1 mL by adding the indicated volumes of carriers. After washing twice, cells were additionally incubated for 47 h and then stained with calcein AM. Then, the stained cells were analyzed using a flow cytometer. Dead cell numbers were estimated by subtracting the viable cell counts from total cell counts.

of an advanced complex carrier for protein delivery by blending the DOPE contained cationic helper lipid with the anionic LP that was used for the conjugation to the Z_{HER2}-BNC. The DOPE contained helper lipid successfully assisted the endosomal escape of the incorporated protein, exotoxin A. The charge of LP was a critical factor in designing the DOPE-containing BNC/LP complex in order to maintain the specificity to HER2-positive breast cancer cells. The optimized blending ratio of the Z_{HER2}-BNC to the DOPE-containing LP mixture dramatically improved the cell-killing activity of the exotoxin A incorporated complex carrier. The conjugation of the LP mixture with the helper lipid should prove to be a useful method for also incorporating virus-like particles to take advantage of their various functions.

Acknowledgements

The authors would like to thank Prof. Shun'ichi Kuroda for his advice on the BNC/LP conjugation method. This work was supported in part by a Special Coordination Fund for Promoting Science and Technology, Creation of Innovative Centers for Advanced Interdisciplinary Research Areas (Innovative Bioproduction Kobe) from the Ministry of Education, Culture, Sports and Technology (MEXT), and Science Research Grants from the Ministry of Health, Labour and Welfare, Japan.

Declaration of interest

The authors report no declaration of interest.

References

Allured VS, Collier RJ, Carroll SF, McKay DB. (1986). Structure of exotoxin A of *Pseudomonas aeruginosa* at 3.0-Angstrom resolution. Proc Natl Acad Sci USA, 83, 1320–1324.

Davison Z, de Blacquière GE, Westley BR, May FE. (2011). Insulin-like growth factor-dependent proliferation and survival of triple-negative breast cancer cells: implications for therapy. Neoplasia, 13, 504–515.

Jia LT, Zhang LH, Yu CJ, Zhao J, Xu YM, Gui JH, Jin M, Ji ZL, Wen WH, Wang CJ, Chen SY, Yang AG. (2003). Specific tumoricidal activity of a secreted proapoptotic protein consisting of HER2 antibody and constitutively active caspase-3. Cancer Res, 63, 3257–3262.

Jung J, Matsuzaki T, Tatematsu K, Okajima T, Tanizawa K, Kuroda S. (2008). Bio-nanocapsule conjugated with liposomes for *in vivo* pinpoint delivery of various materials. J Control Release, 126, 255–264.

Kasuya T, Jung J, Kadoya H, Matsuzaki T, Tatematsu K, Okajima T, Miyoshi E, Tanizawa K, Kuroda S. (2008). *In vivo* delivery of bionanocapsules displaying Phaseolus vulgaris agglutinin-L4 isolectin to malignant tumors overexpressing N-acetylglucosaminyltransferase V. Hum Gene Ther, 19, 887–895.

Kuroda S, Otaka S, Miyazaki T, Nakao M, Fujisawa Y. (1992). Hepatitis B virus envelope L protein particles. Synthesis and assembly in Saccharomyces cerevisiae, purification and characterization. J Biol Chem, 267, 1953–1961.

Lee SB, Hassan M, Fisher R, Chertov O, Chernomordik V, Kramer-Marek G, Gandjbakhche A, Capala J. (2008). Affibody molecules for *in vivo* characterization of HER2-positive tumors by near-infrared imaging. Clin Cancer Res, 14, 3840–3849.

McLarty K, Cornelissen B, Scollard DA, Done SJ, Chun K, Reilly RM. (2009). Associations between the uptake of 111In-DTPA-trastuzumab, HER2 density and response to trastuzumab (Herceptin) in athymic mice bearing subcutaneous human tumour xenografts. Eur J Nucl Med Mol Imaging, 36, 81–93.

Nagai T. (2005). Drug discovery and innovative drug delivery research in new drug development. Pharm Tech Japan, 21, 1949–1951.

Oess S, Hildt E. (2000). Novel cell permeable motif derived from the PreS2-domain of hepatitis-B virus surface antigens. Gene Ther, 7, 750–758.

Orlova A, Magnusson M, Eriksson TL, Nilsson M, Larsson B, Höidén-Guthenberg I, Widström C, Carlsson J, Tolmachev V, Ståhl S, Nilsson FY. (2006). Tumor imaging using a picomolar affinity HER2 binding affibody molecule. Cancer Res, 66, 4339–4348.

Shishido T, Azumi Y, Nakanishi T, Umetsu M, Tanaka T, Ogino C, Fukuda H, Kondo A. (2009a). Biotinylated bionanocapsules for displaying diverse ligands toward cell-specific delivery. J Biochem, 146, 867–874.

Shishido T, Yonezawa D, Iwata K, Tanaka T, Ogino C, Fukuda H, Kondo A. (2009b). Construction of arginine-rich peptide displaying bionanocapsules. Bioorg Med Chem Lett, 19, 1473–1476.

Shishido T, Mieda H, Hwang SY, Nishimura Y, Tanaka T, Ogino C, Fukuda H, Kondo A. (2010). Affibody-displaying bionanocapsules for specific drug delivery to HER2-expressing cancer cells. Bioorg Med Chem Lett, 20, 5726–5731.

Stoeckl L, Funk A, Kopitzki A, Brandenburg B, Oess S, Will H, Sirma H, Hildt E. (2006). Identification of a structural motif crucial for infectivity of hepatitis B viruses. Proc Natl Acad Sci USA, 103, 6730–6734.

Tabata T. (2006). Drug delivery system: Basic technology for biomedical research, medical treatment and health care. Biotechnol J, 6, 553–555.

Yamada T, Iwasaki Y, Tada H, Iwabuki H, Chuah MK, VandenDriessche T, Fukuda H, Kondo A, Ueda M, Seno M, Tanizawa K, Kuroda S. (2003). Nanoparticles for the delivery of genes and drugs to human hepatocytes. Nat Biotechnol, 21, 885–890.

J. Biochem. 2013;153(3):251–256 doi:10.1093/jb/mvs140

JB THE JOURNAL OF BIOCHEMISTRY

Granting specificity for breast cancer cells using a hepatitis B core particle with a HER2-targeted affibody molecule

Received August 30, 2012; accepted October 30, 2012; published online December 11, 2012

Yuya Nishimura[1], Wakiko Mimura[1], Izzat Fahimuddin Mohamed Suffian[1], Tomokazu Amino[1], Jun Ishii[2], Chiaki Ogino[1] and Akihiko Kondo[1,*]

[1]Department of Chemical Science and Engineering, Graduate School of Engineering; and [2]Organization of Advanced Science and Technology, Kobe University, 1-1 Rokkodai, Nada, Kobe 657-8501, Japan

*Akihiko Kondo, Department of Chemical Science and Engineering, Graduate School of Engineering, Kobe University, 1-1 Rokkodai, Nada, Kobe 657-8501, Japan. Tel:/Fax: +81-78-803-6196, email: akondo@kobe-u.ac.jp

Capsid-like particles consisting of a hepatitis B core (HBc) protein have been studied for their potential as carriers for drug delivery systems (DDS). The hollow HBc particle, which is formed by the self-assembly of core proteins comprising 183 aa residues, has the ability to bind to various cells non-specifically via the action of an arginine-rich domain. In this study, we developed an engineered HBc particle that specifically recognizes and targets human epidermal growth factor receptor-related 2 (HER2)-expressing breast cancer cells. To despoil the non-specific binding property of an HBc particle, we genetically deleted the C-terminal 150–183 aa part of the core protein that encodes the arginine-rich domain (ΔHBc). Then, we genetically inserted a Z_{HER2} affibody molecule into the 78–81 aa position of the core protein to confer the ability of target-cell-specific recognition. The constructed Z_{HER2}-displaying HBc (Z_{HER2}-ΔHBc) particle specifically recognized HER2-expressing SKBR3 and MCF-7 breast cancer cells. In addition, the Z_{HER2}-ΔHBc particle exhibited different binding amounts in accordance with the HER2 expression levels of cancer cells. These results show that the display of other types of affibody molecules on HBc particles would be an expandable strategy for targeting several kinds of cancer cells that would help enable a pinpoint DDS.

Keywords: affibody/breast cancer cells/cell-specificity/hepatitis B core/HER2.

Abbreviations: DDS, drug delivery system; FBS, foetal bovine serum; HBc, hepatitis B core; HBV, hepatitis B virus; HER2, human epidermal growth factor receptor-related 2; ΔHBc, HBc deletion mutant lacking arginine-rich domain; SDS–PAGE, sodium dodecyl sulphate–polyacrylamide gel electrophoresis.

Anticancer drugs act against abnormal proteins in cancer cells and present a large treatment effect. However, they are often limited by their systemic toxicities and side effects (*1*). Therefore, targeting ability is an important factor for the development of drug delivery systems (DDS). To attain pinpoint delivery to target cells, studies have extensively focused on fusing targeting molecules with the drug itself (*2*) or on modifying the surface of the DDS carrier (*3*, *4*). As the targeting molecules, binding molecules such as antibodies (*5*), peptides (*6*) and aptamers (*7*) are often used.

As a binding protein, the affibody is an attractive molecule. An affibody is a small molecule that is based on the Z-domain derived from *Staphylococcus aureus* protein A (*8*). As a type of affibody, Z_{HER2} has the ability to bind to human epidermal growth factor receptor-related 2 (HER2) that is a type 2 epidermal growth factor receptor and is expressed on the surface of breast cancer cells and ovarian cancer cells (*9*, *10*). Since natural ligands against HER2 have yet to be found in nature (*11*), Z_{HER2} has been used as an alternative molecular probe to diagnose (*12*) or target HER2-expressing cells (*13*). In addition, various other types of affibodies such as Z_{WT}, Z_{440} and Z_{955} can be used as the binding molecules to the Fc regions of immunoglobulin G, insulin-like growth factor-1 receptor and epidermal growth factor receptor, respectively (*8*, *14*, *15*).

Hepatitis B virus (HBV) core (HBc) protein has been studied for developing viral genome-free particles as DDS carriers. The HBc is a 183-aa protein and assembles spontaneously into icosahedral capsid-like particles comprising 180–240 subunits (*16*). The important feature of HBc is to transiently dissociate and re-associate in the presence or absence of denaturants, thereby enabling it to enclose molecules such as drugs (*17*). In addition, the HBc can be produced in large quantities, because it can be expressed in *Escherichia coli* (*18*). The original HBc has been used as a permeable particle because it has the ability to bind to every cell (*16*), which is caused by an arginine-rich domain (150–183 aa) that recognizes the cell surface heparan sulphate proteoglycan with an electrostatic interaction (*19*). Additionally, foreign molecules (e.g. green fluorescence protein) have been successfully displayed on the surface of a HBc particle without drastically altering its structure via insertion into the 78–81 aa position of the original HBc core protein (*20*).

HBc deletion mutant lacking arginine-rich domain (ΔHBc) consisting of the first 149 aa residues of a core protein was developed as a deletion mutant lacking a non-specific binding ability (*21*). The ΔHBc particle is far more suitable for a DDS capsule than the original HBc because of the particle's capacity to incorporate drugs (*22*) and the avoidance of host-derived RNA/DNA-binding functions (*21*). However, despite the successful development of the ΔHBc particle, there have been no reports of a binding-molecule-fused ΔHBc.

In the present study, we developed a concept for constructing a DDS carrier that is based on the ΔHBc particle and that can specifically recognize target cancer cells. By genetically inserting a Z_{HER2} affibody between the 78 and 81 aa of a ΔHBc core protein, the engineered particle (Z_{HER2}-ΔHBc) specifically bound to HER2-expressing breast cancer cells.

Materials and Methods

Construction of plasmids for the expression of core particles

The plasmids for expression of HBc, ΔHBc and Z_{HER2}-ΔHBc were constructed as described later. Fragments 1 and 2 encoding HBc were amplified by polymerase chain reaction with the following primers: Fragment 1 (5′-GGG GCT AGC AAT AAT TTT GTT TAA CTT TAA GAA GGA GAT ATA CAT ATG ATG GAC ATT GAC CCG TAT AA-3′ and 5′-ATT CTC TAG ACT CGA GAT TAC TTC CCA CCC AGG TGG-3′) and Fragment 2 (5′-TAA TCT CGA GTC TAG AGA ATT AGT AGT CAG CTA TGT-3′ and 5′-CCC GTC GAC TTA GTG GTG GTG GTG GTG GTG ACA TTG AGA TTC CCG AGA TT-3′). Then, the whole-length fragment encoding of HBc was amplified from Fragments 1 and 2 with the following primers: (5′-GGG GCT AGC AAT AAT TTT GTT TAA CTT TAA GAA GGA GAT ATA CAT ATG ATG GAC ATT GAC CCG TAT AA-3′ and 5′-CCC GTC GAC TTA GTG GTG GTG GTG GTG GTG ACA TTG AGA TTC CCG AGA TT-3′). The amplified fragment was digested with NheI/SalI and ligated into the XbaI/SalI sites of pET-22b (+) (Novagen). The resultant plasmid was designated as pET-22b-HBc. Fragment encoding of ΔHBc was amplified from pET-22b-HBc with the following primers: (5′-TAA TCT CGA GTC TAG AGA ATT AGT AGT CAG CTA TGT-3′ and 5′-GGG GTC GAC AAG CTT TTA GTG GTG GTG GTG GTG GTG AAC AAC AGT AGT TTC CGG AA-3′). The amplified fragment was digested with XbaI/SalI and ligated into the same sites of pET-22b-HBc. The resultant plasmid was designated as pET-22b-ΔHBc. A fragment encoding Z_{HER2} was amplified from pGLDsLd50-Z_{HER2} (*23*) with the following primers: (5′-GGG CTC GAG GAC GGT GGT GGT GGT TCT GCG CAA CAC GAT GAA GCC GT-3′ and 5′-GGG TCT AGA ACC ACC ACC ACC TTT CGG CGC CTG AGC ATC AT-3′). The amplified fragment was digested with XhoI/XbaI and ligated into the same sites of pET-22b-ΔHBc. The resultant plasmid was designated as pET-22b-Z_{HER2}-ΔHBc.

Expression of core particles in E. coli

The plasmids for expression of HBc, ΔHBc and Z_{HER2}-ΔHBc were transformed into *E. coli* BL21. The culture of *E. coli* BL21 carrying each plasmid was diluted with 1 l of fresh LB medium (1% tryptone, 0.5% yeast extract, 0.5% NaCl) in the presence of 100 μg/ml ampicillin and grown to $OD_{600} = 0.7$ at 37°C and a shaking speed of 150 rpm. The culture was induced by adding isopropyl-β-thiogalactopyranoside to a final concentration of 0.1 mM at 25°C overnight. Cells were then collected at 3,000 rpm and 4°C for 15 min.

Purification of core particles

To purify core particles fused with a His6-tag, we followed the procedure described by Wizemann and von Brunn (*18*) with minor modifications. Briefly, the cell pellet was re-suspended in 50 ml of lysis buffer (pH 8.0) (50 mM Tris–HCl, 100 mM NaCl, 5 mM EDTA, 0.2% Triton X-100, 10 mM β-mercaptethanol). The cells were lysed on ice by three cycles of sonication for 1 min each with 2-min intervals to avoid heating of the material. The supernatant was removed by centrifugation at 15,000 rpm and 4°C for 30 min. The core particles in the pellet were washed in 50 ml of lysis buffer and collected by centrifugation at 12,000 rpm and 4°C for 15 min twice. The pellet containing *E. coli* proteins was dissolved in 50 ml of dissociation buffer (pH 9.5) (4 M urea, 200 mM NaCl, 50 mM sodium carbonate, 10 mM β-mercaptethanol) by overnight incubation in an ice-cold water bath. Then, the soluble fraction was separated by centrifugation at 15,000 rpm and 4°C for 20 min.

Contaminating proteins were separated from the core particle proteins using Ni^{2+}-chelate affinity chromatography. A column with 10 ml of Ni^{2+}-chelate agarose (Nacalai Tesque, Kyoto, Japan) was pre-equilibrated with a 5-fold volume of dissociation buffer. The prepared sample was loaded into a column and washed with 30 ml of dissociation buffer. Then, bound proteins were eluted with 30 ml of elution buffer (pH 9.5) (4 M urea, 200 mM NaCl, 50 mM sodium carbonate, 10 mM β-mercaptethanol, 1 M imidazole). The eluate was fractionated in 1-ml aliquots. The aliquots of each fraction were subjected to sodium dodecyl sulphate–polyacrylamide gel electrophoresis (SDS–PAGE) and stained with Coomassie brilliant blue to analyse their purity. The proteins of purified fractions were polymerized to core particles by the removal of the urea in a polymerization buffer (pH 7.0) (500 mM NaCl, 50 mM Tris–HCl, 0.5 mM EDTA).

SDS–PAGE and western blotting

The expression of each core monomer was confirmed by western blotting. The purified core particles were analysed by SDS–PAGE and electrotransferred onto a polyvinilidene fluoride membrane. For the detection of the His6-tag, rabbit anti-6-His antibodies (Bethyl Laboratories, Montgomery, TX, USA) were used as a primary antibody for immunoblotting, followed by anti-rabbit antibodies conjugated with alkaline phosphatase (Promega, Madison, WI, USA) used as a second antibody. For the detection of Z protein, Goat anti-protein A antibodies (Rockland Immunochemicals Inc., Gilbertsville, PA, USA) were used as the primary antibody for immunoblotting, followed by anti-goat antibodies conjugated with alkaline phosphatase (Promega) used as the second antibody. The membrane was stained with 5-bromo-4-chloro-3-indolyl phosphate and nitro blue tetrazolium (Promega).

Atomic force microscopy analysis of purified core particles

A gold chip (100-nm thickness of Au wafer; KST world, Fukui, Japan) was covered with 200 μl of solution containing core particles at room temperature for 1 h. The gold chip was then washed with 10 ml of polymerization buffer. After washing, the core particles adsorbed onto the surface of the gold chip were measured using an SPA400-Nanonavi atomic force microscopy unit (SII Nanotechnology Inc., Chiba, Japan) with a cantilever (BL-RC150VB-C1 from Olympus, Tokyo, Japan) at 0.8 kHz scan speed according to the manufacturer's procedure.

Dynamic light scattering analysis of purified core particles

The size of the purified core particles was determined by dynamic light scattering using a Zetasizer Nano ZS (Malvern Instruments Ltd, Worcestershire, UK), following the manufacturer's procedure.

Cell culture

SKBR3 cells (human breast carcinoma) were maintained in RPMI 1640 medium supplemented with 10% (v/v) foetal bovine serum (FBS) at 37°C in 5% CO_2. MCF-7 cells (human breast carcinoma) and HeLa cells (human cervical carcinoma) were maintained in Dulbecco's modified Eagle medium supplemented with 10% FBS at 37°C in 5% CO_2.

Flow cytometric evaluation

Purified core particles were reacted with Alexa Fluor 488 Succinimidyl Esters (Invitrogen Life Technologies, Carlsbad, CA, USA) (2.6 mol equiv) in phosphate-buffered saline for 1 h at room temperature. The mixture then was dialysed against polymerization buffer overnight to remove free Alexa Fluor 488. Approximately 2×10^5 of SKBR3, MCF-7 and HeLa cells were seeded in individual 12-well plates. After washing with serum-free medium, indicated volumes of Alexa Fluore 488-labelled core particles were added to the medium, each of which was adjusted to a volume of 1 ml, followed by culturing of the cells for 1 h. After washing with serum-free medium twice, the cells were incubated with FBS-containing medium

for 2 h. Cells were suspended into a sheath solution and subjected to a BD FACSCanto II flow cytometer equipped with a 488-nm blue laser (BD Biosciences, San Jose, CA, USA). The green fluorescence signal was collected through a 530/30-nm band-pass filter. The data were analysed using the BD FACSDiva software v5.0 (BD Biosciences).

Confocal laser scanning microscopy observation

Approximately 5×10^4 of SKBR3, MCF-7 and HeLa cells were seeded in individual 35-mm glass-bottom dishes. After washing with serum-free medium, Alexa Fluore 488-labelled core particles (10 μg/ml) were added and then cells were cultured for 1 h. After washing with serum-free medium twice, the cells were incubated with FBS-containing medium for 2 h. The cells were observed using a LSM 5 PASCAL laser scanning confocal microscope (Carl Zeiss, Oberkochen, Germany) equipped with a 63-fold oil immersion objective lens with excitation by the 488-nm line of an argon laser and emission collection by a 505-nm long-pass filter.

Results and Discussion

Expression of core proteins and formation of particles

As shown in Fig. 1, we first constructed the plasmid to express the His6-tag-fused HBc, which consisted of 183 aa residues of full-length core proteins. To eliminate the non-specific binding property of a core protein, we constructed the plasmid to express a ΔHBc consisting of 149 aa residues by deleting the corresponding sequence to the C-terminal arginine-rich domain (Fig. 1). Finally, we constructed the expression plasmid for Z_{HER2}-ΔHBc, in which a Z_{HER2} affibody molecule was inserted between the 78 and 81 aa positions of the ΔHBc (Fig. 1). As described in the 'Materials and Methods' section, we introduced these plasmids into *E. coli* and produced each kind of HBc particle.

First, to check the expression and purification of each core protein, we performed western blot analysis with anti-His6 antibody. Since three His6-specific bands appeared at each desired position (HBc, 21 kDa; ΔHBc, 17 kDa and Z_{HER2}-ΔHBc, 24 kDa), successful expression and purification of the core proteins were confirmed (Fig. 2, left). When using anti-protein A antibody that can specifically bind to the Z-derived affibodies, we detected the single band only for Z_{HER2}-ΔHBc (24 kDa), as expected (Fig. 2, right). Furthermore, secondary structural formation of each core protein was confirmed by circular dichroism spectra analysis (data not shown).

Second, to examine whether each core protein-formed particle could be attributed to the capsid-like structure, we analysed the purified core proteins by dynamic light scattering (Fig. 3) and atomic force microscopy (Fig. 4). Two measurement analyses suggested similar results, and it was strongly supported that every core protein showed same particle-like structure that was ~50 nm in diameter. According to previously reported for wild-type HBc particles analysis (*20*, *21*), it was assumed that the deletion of the arginine-rich domain and the insertion of the Z_{HER2} affibody did not affect the self-assembly of the engineered core proteins.

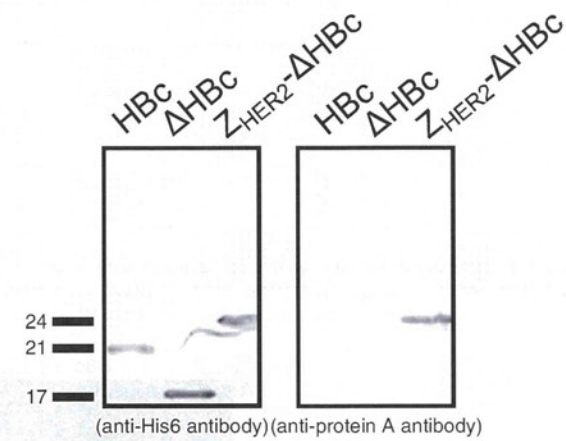

Fig. 2 Western blotting analyses of purified core particles. Purified samples (HBc, ΔHBc and Z_{HER2}-ΔHBc) were subjected to SDS–PAGE followed by immunoblotting using anti-His6 antibody (for His6-tag, left image) and anti-protein A antibody (for Z_{HER2} affibody, right image).

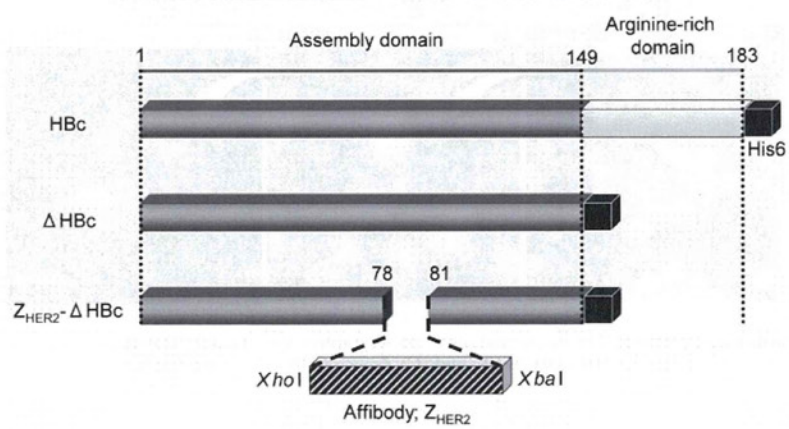

Fig. 1 Schematic representations of constructed core proteins (HBc, ΔHBc and Z_{HER2}-ΔHBc). Wild-type HBc core protein consisted of an assembly domain (grey prismatic body) and an arginine-rich domain (white prismatic body). For ΔHBc core protein, the arginine-rich domain (150–183 aa) was deleted. For the Z_{HER2}-ΔHBc core protein, Z_{HER2} affibody (diagonal prismatic body) was inserted at the XhoI and XbaI sites between 78 and 81 aa. For all constructs, His6-tag (black prismatic body) was fused to the C-termini.

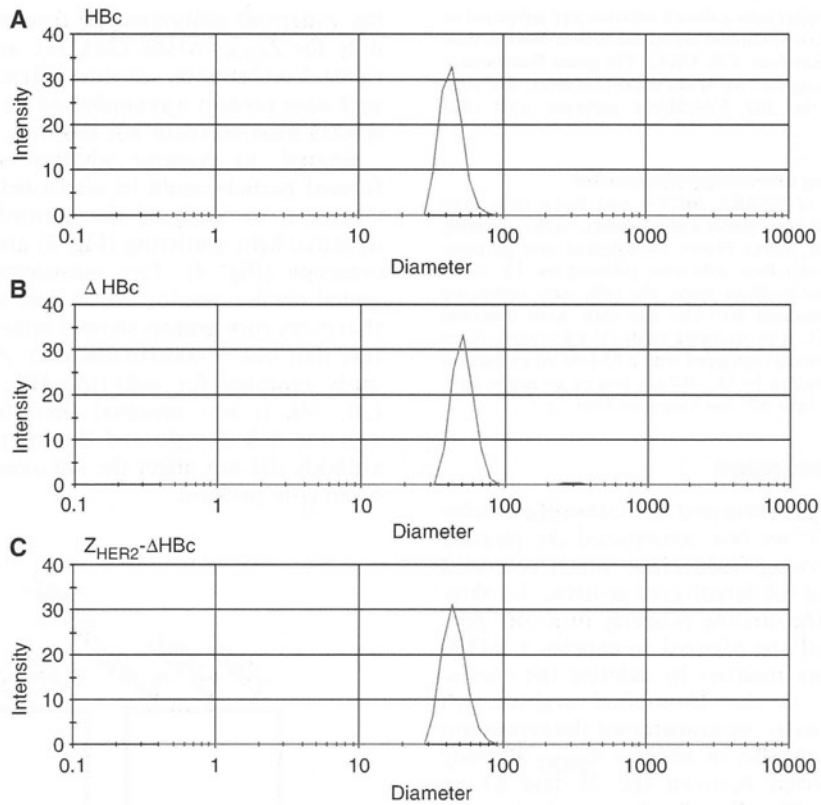

Fig. 3 Particle size distribution analysis by dynamic light scattering. The average sizes of (A) HBc, (B) ΔHBc and (C) Z_{HER2}-ΔHBc are 55.38 ± 10.84 nm, 47.41 ± 10.07 nm and 45.05 ± 1.50 nm, respectively.

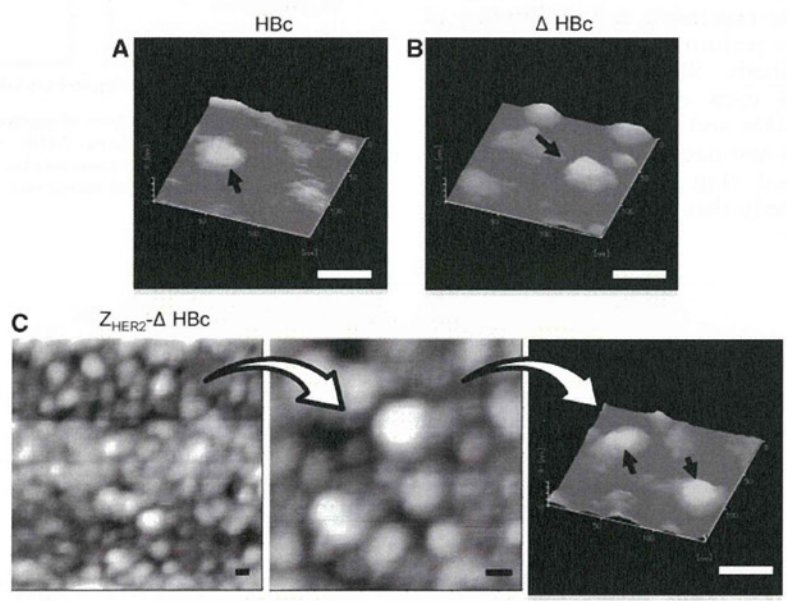

Fig. 4 AFM analyses of purified core particles. The macro and micro photographs show 2D and 3D images, respectively. HBc core particles were analysed on the surface of the gold chip. (A) HBc, (B) ΔHBc and (C) Z_{HER2}-ΔHBc. Scale bars, 50 μm.

Examination of the ability of a Z_{HER2}-ΔHBc particle to recognize HER2-expressing breast cancer cells

Next, to evaluate the binding ability to HER2-expressing breast cancer cells, we labelled the particles with Alexa Fluor 488. Then, each kind of particle was added to two types of HER2-positive human breast cancer cells (SKBR3, expressing an abundant amount of HER2, and MCF-7, expressing a tiny amount of